Published in final edited form as:

Biochim Biophys Acta. 2017 June ; 1863(6): 1157–1170. doi:10.1016/j.bbadis.2017.03.017.

Neurotoxic mechanisms by which the USP14 inhibitor IU1 depletes ubiquitinated proteins and Tau in rat cerebral cortical neurons: relevance to Alzheimer's disease

Magdalena J. Kiprowska[a], **Anna Stepanova**[b,c], **Dustin R. Todaro**[d], **Alexander Galkin**[b,e], **Arthur Haas**[d], **Scott M. Wilson**[f], and **Maria E. Figueiredo-Pereira**[a,*]

[a]Department of Biological Sciences, Hunter College, Biology and Biochemistry Programs, Graduate Center, The City University of New York, New York, NY 10065, USA

[b]School of Biological Sciences, Queen's University Belfast, Belfast, BT9 7BL, United Kingdom

[c]N.K. Koltzov Institute of Developmental Biology, Russian Academy of Sciences, Moscow 119334, Russia

[d]Department of Biochemistry and Molecular Biology, LSU Health Sciences Center, New Orleans, LA 70112, USA

[e]Feil Family Brain and Mind Research Institute, Weill Cornell Medical College, New York, NY 10065, USA

[f]Department of Neurobiology, Civitan International Research Center, University of Alabama at Birmingham, Birmingham, AL 35294

Abstract

In Alzheimer's disease proteasome activity is reportedly downregulated, thus increasing it could be therapeutically beneficial. The proteasome-associated deubiquitinase USP14 disassembles polyubiquitin-chains, potentially delaying proteasome-dependent protein degradation. We assessed the protective efficacy of inhibiting or downregulating USP14 in rat and mouse (*Usp14*$^{ax.J}$) neuronal cultures treated with prostaglandin J2 (PGJ2). IU1 concentrations ($_{H}$IU1 >25 μM) reported by others to inhibit USP14 and be protective in non-neuronal cells, reduced PGJ2-induced Ub-protein accumulation in neurons. However, $_{H}$IU1 alone or with PGJ2 is neurotoxic, induces calpain-dependent Tau cleavage, and decreases E1~Ub thioester levels and 26S proteasome assembly, which are energy-dependent processes. We attribute the two latter $_{H}$IU1 effects to ATP-deficits and mitochondrial Complex I inhibition, as shown herein. These $_{H}$IU1 effects mimic those of mitochondrial inhibitors in general, thus supporting that ATP-depletion is a major mediator of $_{H}$IU1-actions. In contrast, low IU1 concentrations ($_{L}$IU1 ≤25 μM) or USP14 knockdown by siRNA in rat cortical cultures or loss of USP14 in cortical cultures from *ataxia* (*Usp14*$^{ax.J}$) mice, failed to prevent PGJ2-induced Ub-protein accumulation. PGJ2 alone induces Ub-protein accumulation and decreases E1~Ub thioester levels. This seemingly paradoxical result may be attributed to PGJ2 inhibiting some deubiquitinases (such as UCH-L1 but not USP14), thus

*Corresponding Author: Maria E. Figueiredo-Pereira, Department of Biological Sciences, Hunter College and Graduate Center, City University of New York, 695 Park Ave., New York, NY 10065, USA, Tel.: 212-650-3565; Fax: or 212-772-5227; pereira@genectr.hunter.cuny.edu.

triggering Ub-protein stabilization. Overall, IU1-concentrations that reduce PGJ2-induced accumulation of Ub-proteins are neurotoxic, trigger calpain-mediated Tau cleavage, lower ATP, E1~Ub thioester and E1 protein levels, and reduce proteasome activity. In conclusion, pharmacologically inhibiting (with low or high IU1 concentrations) or genetically down-regulating USP14 fail to enhance proteasomal degradation of Ub-proteins or Tau in neurons.

Keywords

Alzheimer's; deubiquitinase; ubiquitin-activating enzyme; USP14; mitochondria; Tau; calpain

1. Introduction

The ubiquitin/proteasome pathway (UPP) and autophagy play a critical role in protein quality control and thus have attracted special attention for drug development [17]. Alzheimer's disease (AD) is of particular interest since a hallmark of this neurodegenerative disorder is accumulation/aggregation of Ub-proteins in specific areas of the CNS [67]. A potential therapeutic strategy for AD could be directed towards deubiquitinases to prevent the accumulation and aggregation of Ub-proteins [13].

In humans there are around one hundred genes encoding deubiquitinases from five different families, four of them being thiol proteases and one a metalloprotease [18]. Deubiquitinases perform a range of functions, including processing newly translated ubiquitin (Ub) to provide monomers for conjugation and chain formation, trimming mono-Ub from the distal end of a poly-Ub chain, disassembling poly-Ub chains, and removing poly-Ub chains from substrates [11]. Overall, these functions provide a means for deubiquitinases to regulate "where, when and why" ubiquitinated substrates are degraded by the 26S proteasome [67].

The deubiquitinase USP14 is required for the development and functioning of the nervous system [9,12,79,84]. Mice homozygous for the *ataxia* mutation (ax^J, 95% USP14 loss) exhibit developmental abnormalities including motor impairment, reduced brain mass and death by two months of age [14]. USP14 associates transiently with the proteasome and exhibits Ub-chain trimming activity, thereby replenishing the Ub pool [6,9,44]. This deubiquitinase can cause premature dissociation of substrates from the proteasome, if ubiquitin removal is faster than the competing steps leading to substrate degradation [6,44]. Inhibiting or downregulating USP14 was proposed as a therapeutic approach for promoting the efficient proteasomal elimination of Ub-proteins by preventing premature trimming of their Ub-chains [44].

Selective and reversible inhibition of USP14 can be achieved with 1-[1-(4-Fluoro-phenyl)-2,5-dimethyl-1H-pyrrol-3-yl]-2-pyrrolidin-1-yl-ethanone, a small molecule known as IU1 [44]. Treatment of murine embryonic fibroblasts (MEFs) and human embryonic kidney (HEK)293 cells with IU1 resulted in the apparent increased degradation of the proteasome substrates Tau, TDP-43 and ataxin-3, which have been implicated in neurodegenerative diseases [44]. These studies suggest that IU1 or IU1-like drugs could be used therapeutically to prevent the neurotoxic build-up of such proteins in neurons.

To test whether IU1 prevents accumulation of neuronal Ub-proteins, we treated rat and mouse cerebral cortical neurons with the endogenous product of inflammation prostaglandin J2 (PGJ2) [22]. PGJ2 is a product of spontaneous dehydration of prostaglandin D2 (PGD2). PGD2 is the most abundant prostaglandin in the brain [30,71,78] and the one that increases the most under pathological conditions [47]. In rodents, the *in vivo* concentration of free PGJ2 in the brain upon stroke and traumatic brain injury increases from almost undetectable to the 100 nM range [49,50]. These values represent average brain levels. Regional brain concentrations of PGJ2 are potentially higher [51], as PGJ2 binds covalently to proteins, and therefore free PGJ2 does not represent its total amount. Unlike most prostaglandins, PGJ2 and its metabolites have a cyclopentenone ring with reactive α,β-unsaturated carbonyl groups. These carbonyl groups form covalent Michael adducts with cysteine thiols of glutathione or cellular proteins [76]. Electrophiles, such as PGJ2, that bind to specific protein cysteine(s) are regarded to play an important role in determining neuronal survival [69].

We previously established that PGJ2 is the most toxic of four prostaglandins that we tested in neuronal cells, including PGA1, D2, E2 and J2 [46]. In addition, PGJ2 impairs the UPP by targeting different components of this pathway including the 26S proteasome by perturbing its assembly [60,82], some deubiquitinases such as UCH-L1 and Ub isopeptidase activities [40,46,49,57] (not USP14 as we show herein), and by causing the accumulation/aggregation of Ub-proteins [46,50]. Besides its effects on the UPP, we showed that PGJ2 induces activation of caspases and caspase-mediated proteolysis in primary cerebral cortical neuronal cultures, leading to Tau cleavage and pathology [2,55]. In sum, PGJ2 induces a range of pathological processes relevant to neurodegenerative disorders such as AD (see [22] for a discussion on the relevance of PGJ2 and its precursor PGD2 to AD).

In the current study we demonstrate that concentrations of IU1 ($_{H}$IU1 >25 μM) reported to effectively inhibit USP14 and to be protective in non-neuronal cells [44], deplete the accumulation of Ub-proteins in rat cerebral cortical neuronal cultures treated with PGJ2. However, this effect of $_{H}$IU1 is not attributable to increased proteasome activity, but instead to a decline in E1~Ub thioester and E1 protein levels, correlating with a drop in ATP levels and mitochondrial Complex I activity. $_{H}$IU1 was also neurotoxic and induced calpain-dependent cleavage of Tau, spectrin and caspase. Overall, the effects of $_{H}$IU1 on neuronal Ub-protein levels, E1- and calpain-activities, Tau cleavage and ATP levels, mimic those of mitochondrial inhibitors such as oligomycin, antimycin and rotenone [35]. Lower IU1 concentrations ($_{L}$IU1 ≤25 μM), or downregulating USP14 by siRNA, or loss of USP14 (*Usp14*^{axJ} mouse) did not significantly decrease Ub-protein levels. We also established that PGJ2 lowers E1~Ub thioester levels without directly inhibiting E1 activity. In contrast to IU1, PGJ2 induces the accumulation of Ub-proteins in neuronal cultures, but does not inhibit USP14. In conclusion, a deeper understanding of the mechanisms that regulate Ub-protein accumulation, including the balance among E1, deubiquitinase and proteasome activities, is critical for drug development that aims at reducing the abnormal accumulation of Ub-proteins in the CNS of patients with AD and other chronic neurodegenerative diseases.

2. Materials and Methods

2.1. Materials

Chemicals: IU1 (Life Sensors, Malvern, PA); calpeptin (Calbiochem/EMD Bioscience, Gibbstown, NJ); proteasome substrate Suc-LLVY-AMC (BACHEM Bioscience Inc., King of Prussia, PA); HA-Ub-VME (ENZO Life Sciences, Inc., Farmingdale, NY); PGJ2 (Cayman Chemical, Ann Arbor, MI); oxidative phosphorylation substrates, creatine phosphokinase, and bovine ubiquitin (Sigma-Aldrich, St. Louis, MO). Primary antibodies: Chicken polyclonal anti-USP14 (1:1,000, cat# AB505) from Life Sensors, Malvern PA or as in [1]; rabbit polyclonal anti-ubiquitinated proteins (1:1,500, cat# Z0458) from Dako North America, Carpinteria, CA; mouse monoclonal anti-HA (1:1,000, cat# 12CA5) from Roche (Indianapolis, IN); rabbit polyclonal anti-β5 (1:5,000, cat# PW8895), and mouse monoclonal anti-Rpt6 (1:2,000, cat# PW9265), from ENZO Life Sciences, Inc., Farmingdale, NY; mouse monoclonal anti-β-actin (1:10,000, cat# A-2228) from Sigma, St. Louis, MO; mouse monoclonal anti-spectrin α chain (clone AA6, cat# MAB1622) from Millipore, Billerica, MA; mouse monoclonal Tau C3 (1:5,000; detects Tau cleaved at Asp421; ep: a.a. 412–421) and mouse monoclonal Tau C5 (1:50,000; detects all Tau isoforms and ΔTau; ep: a.a. 210–241) were courtesy of Dr. L. Binder (Northwestern University, Chicago, IL, USA); rabbit polyclonal anti-UBE1a (1:1000, cat# 4890) and anti-caspase 3 (1:1000, cat# 9662) from Cell Signaling Technology, Danvers, MA. Secondary antibodies with HRP conjugate (1:10,000) from Bio-Rad Laboratories, Hercules, CA.

2.2. Mice

C57BL/6J (wild type) and *Usp14*^{axJ} mice maintained on a C57BL/6J background (Jackson Laboratories, Bar Harbor, MA) have been maintained in the breeding colony at the University of Alabama at Birmingham. Homozygous *Usp14*^{axJ} mice were generated by intercrossing heterozygous *ax*^{J} siblings.

2.3. Cell cultures

Dissociated cultures from Sprague Dawley rat embryonic (E18, both sexes) cerebral cortical neurons were prepared as in [35]. Dissociated cultures from wild type and homozygous *Usp14*^{axJ} mouse embryos were prepared as in [15]. The isolated cortices free of meninges were digested with papain (0.5 mg/ml from Worthington Biochemical Corp.) in Hibernate E without calcium (BrainBits LLC.) at 37°C for 30 min in a humidified atmosphere containing 5% CO_2. After removal of the enzymatic solution, the tissues were gently dissociated in Neurobasal media (Invitrogen). Dissociated tissues were centrifuged at 300×*g* for 2 min. The pellet was resuspended in Neurobasal media without antibiotics and plated on 10 cm dishes pre-coated with 50 μg/mL poly-D-lysine (Sigma). Cells were plated at a density of 6×10^6 cells per 10 cm dish, or 2.5×10^5 cells per well on 24-well plates (cell viability only). Cultures were maintained in Neurobasal media supplemented with 2% B27 and 0.5 mM L-Glutamax (all from Invitrogen) at 37°C in a humidified atmosphere containing 5% CO_2. Half of the medium was changed every 4 days. Experiments were run 8–11 DIV. According to manufacturer's specifications, Neurobasal medium contains several proprietary factors that ensure a mostly pure (> 95%) neuronal culture; glial growth is inhibited without a need for the anti-mitotic agent arabinofuranosyl cytidine [8,59].

2.4. Culture treatments

Cortical neurons were treated acutely (4 h, 8 h, 16 h or 24 h) with DMSO or with the different drugs in DMSO added directly to DMEM without serum, supplemented with 0.5 mM L-Glutamax and 1 mM sodium pyruvate (all from Invitrogen). The final DMSO concentration in the medium was 0.5%.

2.5. Cell viability assay

Cell viability was assessed with the 3-(4,5-dimethylthiazol-2-yl)-2,5-diphenyl tetrazolium bromide (MTT) assay as described [56].

2.6. ATP assay

Steady state ATP content was measured with a kit using the sensitive luciferin/luciferase system (Molecular Probes). This assay is based on luciferase requiring ATP for light production using luciferin as a substrate. Cells were harvested with 4% trichloroacetic acid followed by centrifugation (19,000×*g*, 15 min at 4°C). ATP steady state levels were determined in cleared supernatants after neutralizing the samples with 1 M Tris-HCl, pH 8.0. Samples were then added to the reaction buffer containing luciferin and assayed using a Luminoskan Ascent microplate luminometer (Thermo Electron Corporation). Protein concentration was determined with the bicinchoninic acid (BCA) assay kit (Pierce) after resuspending the pellet in 10 mM Tris-HCl (pH 8.0) and 1% SDS followed by sonication. ATP levels were normalized to protein concentration determined with the BCA assay.

2.7. Mitochondrial respiratory chain complex activities

Rat brain mitochondria were prepared according to a standard protocol with Percoll gradient centrifugation [10]. For individual respiratory chain complex activity assessment, mitochondria were resuspended to approximately 2–5 mg/ml in SET buffer pH 7.5 (0.25 M sucrose, 0.2 mM EDTA, 50 mM Tris-HCl), containing 0.2 mM malonate and incubated at 30°C for 30 min for activation of complex II [75]. NADH-dependent enzymatic activities of Complex I were assayed spectrophotometrically (Perkin Elmer Lambda 35) as a decrease in absorption at 340 nm (ε_{340} nm = 6.22 mM^{-1} cm^{-1}) with 150 μM NADH in the SET buffer supplemented with 40 μg/ml alamethicin and containing 2.5–25 μg of protein/ml mitochondria. For the measurements of NADH:Q_1 or NADH:HAR oxidoreductase activity, mitochondrial membranes were assayed in the presence of 1 mM cyanide with the addition of 80 μM Q_1 or 1 mM HAR, respectively. The Complex IV activity was measured at 550 nm (ε_{550}nm = 21.5 mM^{-1} cm^{-1}) with 45 μM ferrocytochrome *c* in two fold diluted SET buffer containing 0.025% laurilmaltoside and 2.5–5 μg of protein/ml mitochondria.

To measure the effect of IU1 on respiratory chain enzymes, mitochondrial membranes were preincubated directly in the measuring medium for 2 min with the inhibitor before initiating the reaction with a substrate. Separate control studies confirmed the preincubation time was sufficient to reach equilibrium in the enzyme-inhibitor reaction.

Succinate-oxidase (5 mM succinate and 1 mM glutamate) or Complex I-dependent respiration (2mM malate and 2 mM glutamate) of freshly prepared intact mitochondria were performed using the Oroboros respirometer as described previously [75]. 0.5 mM ADP was

used for initiation of state 3 respiration and estimation of the ADP/O ratio. ATP synthase activity was assessed in rat brain intact mitochondria by determining the ADP/O ratio on succinate oxidase.

All activities were measured at 30°C and expressed in μmol of substrate×min^{-1}×mg^{-1}. Protein concentration was determined with the BCA assay. Reported values are the mean ± SD (at least 3 independent experiments). Similar results were obtained with heart mitochondria.

2.8. Western blotting

After treatment, cells were rinsed twice with PBS and harvested by gently scraping into ice-cold lysis buffer [20 mM Tris-HCl, pH 7.5, 137 mM NaCl, 1 mM EGTA, 2.5 mM $Na_4P_2O_7$, 1 mM β-glycerophosphate, 50 mM NaF, 1 mM phenylmethylsulfonyl fluoride, 1% NP40, 1 mM Na_3VO_4, 1% Glycerol and protease inhibitor cocktail (Sigma-Aldrich, St Louis, MO)]. Following lysis (at least 30 min, −80°C), cell extracts were centrifuged (19,000×g for 10 min) at 4°C. Protein concentration of the NP40-soluble supernatants were determined with the BCA assay. Western blot analysis was carried out following SDS-PAGE. Normalized samples were boiled for 5 min in Laemmli buffer and loaded onto gels (30 μg of protein/lane). Following electrophoresis, proteins were transferred onto an Immobilon-P membrane (Millipore, Bedford, MA, USA). The membrane was probed with the respective antibodies, and antigens were visualized by a standard chemiluminescent horseradish peroxidase method with the ECL reagent. Semi-quantitative analysis of protein detection was done by densitometry including image analysis with the ImageJ program (Rasband, W.S., ImageJ, U.S. NIH, Maryland, http://rsb.info.nih.gov/ij/, 1997–2006).

2.9. Evaluation of endogenous E1~ubiquitin thioester

Upon treatment with vehicle (control, DMSO) or with the respective drugs, cortical neurons were washed once with PBS, harvested with a thiol stabilizing buffer [5 mM Tris-HCl, pH 7.8, 8.7 M urea, 1% Nonidet P-40, 20 mM N-ethylmaleimide, 3 mM EDTA, 2% protease inhibitor cocktail (Sigma)], and kept on ice for 15 min for lysing, as described [38]. Samples were sonicated for 10 s, centrifuged at 19,000×*g* for 15 min at 4°C, mixed (30 μg) 1:2 (volume) with thioester gel buffer (33 mM Tris-HCl, pH 6.8, 2.7 M urea, 2.5% SDS and 13% glycerol), and boiled for 5 min. After determination of the protein concentration with the Bradford assay (Bio-Rad Laboratories), the normalized samples were separated into reducing (with 4% β-mercaptoethanol) and non-reducing (no β-mercaptoethanol) aliquots for SDS-PAGE, followed by western blotting with anti-E1 antibody, as described above.

2.10. In vitro E1 activity assay

Commercial bovine ubiquitin was further purified to apparent homogeneity by FPLC and quantified spectrophotometrically [3]. Ubiquitin was radioiodinated by the Chloramine-T procedure using carrier-free $Na^{125}I$ to yield a specific radioactivity of ~20,000 cpm/pmol [29]. Human Uba1 (E1) was purified to apparent homogeneity from outdated erythrocytes and active Uba1 was determined by the stoichiometric formation of ^{125}I-ubiquitin thioester [29]. One pmol of Uba1 was pre-incubated with 0.5% DMSO (vehicle) or 15 μM PGJ2 (0.5% DMSO) at 4°C in 50 mM Tris-HCl (pH 7.5) for 0, 1, 2, 4, 6, 12, and 24 hours.

Formation of E1 thioester was analyzed at 37°C in 25 μl reactions containing 50 mM Tris-HCl (pH7.5), 1 mM ATP, 10 mM $MgCl_2$, 10 mM creatine phosphate, 1 IU of creatine phosphokinase and an aliquot of the time point equivalent to 40 nM Uba1 (original content). Reactions were started by the addition of 4 μM ^{125}I-ubiquitin and quenched after 1 min by the addition of 25 μl 2× SDS sample buffer. The E1~^{125}I-ubiquitin thioesters were resolved from free ^{125}I-ubiquitin by 12% SDS-PAGE under non-reducing conditions at 4°C and visualized by autoradiography. Where indicated, E1 was quantified by excising the E1~^{125}I-ubiquitin thioester band, quantifying associated radioactivity by gamma counting, and calculating absolute thioester formation using the corrected specific radioactivity of the ^{125}I-ubiquitin [29].

2.11. In vitro assay for USP14 enzymatic activity

The ubiquitin hydrolase activity of USP14 is activated when associated with the 26S proteasome [33]. USP14 activity was assessed as previously described [1] using HA-tagged ubiquitin vinyl methyl ester (HA-Ub-VME), which is an active site-directed probe that irreversibly modifies a subset of DUBs including USP14 [7]. Briefly, 5 μg of wild type mouse brain proteasomes were diluted in a solution containing 50 mM Tris, pH 7.5, 250 mM sucrose, 1 mM DTT and 2 mM ATP. To measure active USP14, reactions were started by adding HA-Ub-VME (0.2 μg) in the absence or presence of increasing PGJ2 concentrations (10 μM to 100 μM) and incubated at 23°C for 30 min. Reactions were stopped by adding SDS sample buffer and boiling for 5 min. Samples were run on SDS-PAGE followed by western blotting with the anti-HA antibody as described above.

2.12. In gel proteasome activity and levels

Upon treatment with vehicle (control, DMSO) or the respective drugs, cells were washed twice with PBS and harvested for the in gel assay as described in [58]. The native gels loaded with 30 μg protein/lane, were run at 150 V for 120 min. The in gel proteasome activity was detected by incubating the native gel on a rocker for 10 min at 37°C with 15 ml of 300 μM Suc-LLVY-AMC followed by exposure to UV light (360 nm). Gels were photographed with a NIKON Cool Pix 8700 camera with a 3–4219 fluorescent green filter (Peca Products, Inc). Proteins on the native gels were transferred (110 mA) for 2 h onto PVDF membranes. Immunoblotting was carried-out for detection of the 20S and 26S proteasomes with the anti-Rpt6 and anti-β5 antibodies, which react with subunits of the 19S or the 20S particles, respectively. Antigens were visualized by a chemiluminescent horseradish peroxidase method with the ECL reagent.

2.13. Caspase-3 and calpain activation

Cell lysates were analyzed by standard western blotting with the anti-caspase-3 antibody to detect caspase-3 cleavage that is indicative of apoptosis. Calpain activation was assessed with the anti-α-spectrin antibody. Calpain cleavage of α-spectrin generates a 150/145 kDa doublet, while caspase cleavage generates a 120 kDa fragment [81].

2.14. siRNA

The dicer siRNA substrates targeting the *USP14* gene obtained from IDT (Coralville, Iowa), were encapsulated into lipid nanoparticles using microfluidic technology by Precision NanoSystems (SUB9KITS™; Vancouver, Canada). Cells were treated with 0.1 μg/ml of Neuro9™ RNAi nanoparticles as described in [68] for 72 h prior to treatment with 10 μM PGJ2 for 16 h. During siRNA treatment, cells remained in Neurobasal media supplemented with 2% B27 and 0.5 mM L-Glutamax (all from Invitrogen) at 37°C in a humidified atmosphere containing 5% CO_2. Following the 72 h incubation period with siRNA, the medium was changed to DMEM without serum, supplemented with 0.5 mM L-Glutamax and 1 mM sodium pyruvate (all from Invitrogen) and cells were treated with 10 μM PGJ2 for 16h.

2.15. Mass Spectrometry

Cortical neurons from E15 C57Bl/6J mouse embryos were seeded at a density of 5.0×10^5 cells per well. Following seven days in culture, neurons were treated with 20 μM or 100 μM IU1 for 24 hours. Cells were then washed three times in PBS to remove any extracellular IU1 and lysed in 10 mM Tris (pH 7.5), 1 mM EDTA, 0.5 mM EGTA, 1% Triton X-100, 0.5% SDS and 140 mM NaCl buffer. IU1 concentrations were determined by the UAB Targeted Metabolomics and Proteomics Laboratory using Liquid Chromatography-Multiple Reaction Monitoring Mass Spectrometry. For chromatography, a Synergi Polar-RP 2.5μ 50 × 2.0 mm size (Phenomenex, Torrance, CA) was used at 50°C. Mobile phases A and B were *dd*H_2O with 0.1% formic acid and methanol with 0.1% formic acid, respectively. Analytes were eluted with a linear 5–100% gradient of B over 3 minutes, 100% B for 0.5 minutes, a return to 5% B in 0.1 minutes, and re-equilibration for 1.4 minutes at starting conditions (5% B) at a flow rate of 500 μL/min. The SCIEX 4000 triple quadrupole mass spectrometer (SCIEX, Foster City, CA) analyzed IU1 containing samples in the positive ion mode. Electrospray ionization voltage was set to 4500 V. Curtain gas, GS1, and GS2 were set at 20, 60, and 60 PSI, respectively, with an interface heater setting of 450°C. The parent and daughter ion combination for detection of IU1 were the following: m/z 301.3 → 84.1 using a collision energy of 35 eV, declustering potential of 56 V, entrance potential of 11 V, and exit potential of 4 V. Data were analyzed utilizing MultiQuant 2.1.1 (SCIEX, Foster City, CA) for calculating unknown IU1 concentrations against a standard curve of known amounts of IU1.

2.16. Statistical analysis

Statistical significance was estimated using one-way ANOVA (Tukey's multiple comparison test) with the Prism 6 program (GraphPad Software, San Diego, CA).

3. Results

3.1. IU1 blocks PGJ2-induced accumulation of ubiquitinated proteins and triggers calpain-mediated cleavage of Tau, caspase 3 and spectrin

Since IU1 was proposed to enhance protein degradation by the proteasome [44] we examined its effects on neuronal Ub-protein levels. IU1 was not previously tested on

neurons [44]. To increase the endogenous levels of Ub-proteins, the rat cerebral cortical neuronal cultures were treated with the product of inflammation PGJ2 [74,78]. Neurons were pre-incubated with IU1 (75 μM) for 6 h prior to PGJ2 treatment (15 μM, 16 h). A similar protocol was used to establish protection by IU1 against proteotoxic stress in HEK293 cells treated with menadione, an oxidative stressor [44]. We investigated the effects of PGJ2 and IU1 alone or combined on Ub-protein levels and quantified the results as Ub/actin ratios. As expected and shown in Figure 1, PGJ2 significantly increased the levels of Ub-proteins (*lane 2, panels 1 and 2, n=4, *p = 0.015*). Although 75 μM IU1 by itself did not decrease Ub-protein levels (*compare lanes 1 and 3, n=4, p=0.95*), IU1 reduced the accumulation of Ub-proteins induced by PGJ2 (*compare lanes 2 and 4, n=4, p=0.0014*).

IU1 was previously shown to enhance the degradation of a Tau isoform overexpressed in wild type MEFs [44]. Tau is a microtubule associated protein that is abundant in neurons and highly soluble, yet Tau forms abnormal aggregates and is the major component of neurofibrillary tangles, one of the hallmarks in AD [53]. Confirming what we previously demonstrated [55], PGJ2 induced caspase-mediated cleavage of Tau (ΔTau, Fig. 1, panel 4, lane 2). ΔTau is prone to aggregation and its formation is an early event in AD tangle pathology [16,24,66]. In contrast to PGJ2, IU1 induced calpain-mediated cleavage of Tau (Fig. 1, panel 3, lane 3), reminiscent of what we observed in cortical neurons treated with the mitochondrial inhibitors oligomycin, antimycin and rotenone [35]. IU1 combined with PGJ2 further increased calpain-mediated cleavage of Tau (Fig. 1, panel 3, lane 4).

We established that IU1-treatment induces calpain activation, while PGJ2-treatment triggered mostly caspase 3 activation. As shown in Fig. 1 (*panel 5, lane 3*), IU1 triggered the cleavage of pro-caspase 3 to a ~29 kDa inactive fragment [61] (Cl-caspase 3) and not to its active 17 kDa form (Act-caspase 3). On the other hand, PGJ2 induced the cleavage of pro-caspase 3 (33 kDa) to its active form (17 kDa, Act-caspase 3, Fig. 1, panel 5, lane 2), as we previously showed [2]. We further confirmed that calpain was activated upon IU1-treatment by assessing cleavage of α-spectrin, a calpain substrate. IU1-treatment by itself or in combination with PGJ2 clearly induced cleavage of α-spectrin (Pro-α-spectrin, 280 kDa) to 145/150 kDa fragments [Cl-α-spectrin (150)], which are indicative of calpain activation (Fig. 1, panel 6, lanes 3 and 4). In contrast, PGJ2-treatment mostly induced α-spectrin cleavage to a 120 kDa α-spectrin fragment [Cl-α-spectrin (120)], which is a marker of apoptotic cell death [81]. Furthermore, pre-treatment with the calpain inhibitor calpeptin (Z-Leu-norleucinal) prevented calpain-dependent Tau and spectrin cleavages induced by IU1 alone (Fig. 1, panels 3 and 6, compare lanes 3 and 6). In contrast, treatment with both calpeptin and IU1 stimulated caspase-dependent Tau cleavage the most (Fig. 1, panel 4, lane 6), indicating caspase activation under these conditions as discussed below.

We next addressed if lower IU1 concentrations (≤ 25 μM) also blocked the accumulation of Ub-proteins induced by PGJ2. Since PGJ2 has dose-dependent effects [2,55], for these experiments we reduced the PGJ2 concentration to 10 μM, as we also lowered IU1 levels. Adding IU1 to the neuronal cultures prior to PGJ2-treatment had the same effect as co-incubation with the two drugs (*not shown*). Therefore, in all subsequent experiments both agents were added at the same time. We established that for the 4 h and 24 h time points 25 μM IU1 did not change the levels of Ub-proteins detected in control or PGJ2-treated neurons

(Fig. 2A for 4h, n=3, and Fig. 2B for 24h, n=4). The quantification measuring Ub/actin ratios and the *p* values (non-significant) are shown in Figure 2C. We also determined for the 4 h time point that 1 μM, 5 μM, and 10 μM IU1 did not deplete the levels of Ub-proteins detected in control or PGJ2-treated neurons (Fig 2A, n=4). For these latter conditions, the *p* values determined by comparing Ub-protein levels in control or PGJ2-treated neurons with those when IU1 was added were ≥0.2, thus non-significantly different. While the lanes corresponding to 1 μM and 5 μM IU1 treatment may show a trend toward increased ubiquitin conjugates, as explained above there is no significant effect of IU1 at low levels with co-treatment or pre-treatment (the latter not shown).

Finally, mass spectrophometry analysis of cells treated with 20 μM or 100 μM IU1, revealed an approximately 19.58 μM and 90 μM IU1 intracellular concentration, respectively.

3.2. IU1 reduces cell viability and depletes intracellular ATP levels

Calpain-activation is linked to ATP-depletion and necrosis, a cell death pathway associated with a bioenergetic crisis [86]. In fact, calpain-activation was shown to be induced by inhibitors of oxidative phosphorylation, such as rotenone, antimycin and oligomycin [73]. As we established that IU1 induces calpain activation, we reasoned that IU1 may be neurotoxic and lower intracellular ATP levels.

As shown in Fig. 3, IU1 caused a decline in cell viability in a concentration (*panel A*) and time-dependent-manner (*panel B*), the latter assessed for 25 μM. A concentration of IU1 as low as 5 μM was significantly neurotoxic (*n=12, p=0.005*). In addition, treatment with PGJ2 (10 μM) and IU1 (25 μM) combined was even more neurotoxic than any of the drugs alone (*panel C, comparing IU1 with IU1+PGJ2, p=0.03*). The loss of neuronal viability was assessed with the MTT assay, which is reduced largely within the cytoplasm [5,52].

As we predicted, IU1 decreased ATP levels also in a concentration (Fig. 4A) and time-dependent manner (Fig. 4B). Moreover, treatment with PGJ2 (10 μM) combined with IU1 (25 μM) decreased ATP levels the most, compared to the effectiveness of either compound alone (*panel C*).

The decline in ATP levels induced by the 24h treatment with 25 μM IU1 varied between 70% (Fig. 4B) and 90% (Fig. 4A) of control. The loss of cell viability under the same conditions fluctuated more, between 40% (Fig. 3 A and B) and 80% (Fig. 3C) of control. The finding that neurons that exhibit a 70% to 90% loss of ATP still exhibit low levels of viability is in line with other studies. For example, we showed that 30% of oligomycin-treated rat cortical neurons exhibiting a loss of ~78% of their ATP were still viable [35].

3.3. IU1 inhibits mitochondrial Complex I from rat brain

As shown in Fig. 5, NADH-oxidase (*A*) and NADH:Q_1 reductase (*B*) activities of Complex I were inhibited by IU1, the latter with an IC50 of around 40 μM. This indicates a direct effect of IU1 on physiological oxidation of NADH by ubiquinone in mitochondrial Complex I. At a much higher concentration IU1 also inhibited oxidation of NADH by the artificial acceptor hexaammineruthenium (HAR, *C*). In addition, at this concentration range IU1 had almost no effect on succinate dehydrogenase (Complex II, *D*) or on cytochrome *c* oxidase alone

(Complex IV, *E*). Similar results were obtained with SMPs isolated from heart tissue (not shown). When measuring state3/state oxygen consumption of intact mitochondria, the ADP/O ratio of ~1.5 on succinate-supported respiration did not change in the presence of 300 μM IU1, indicating that the inhibitor does not directly affect complex V or ATP synthase.

3.4. The IU1-induced decline in Ub-proteins upon PGJ2-treatment correlates with lower E1~Ub thioester and E1 protein levels

To address a mechanism mediating the IU1-induced decline in Ub-protein accumulation, we focused on the E1 ubiquitin activating enzyme. E1 activity requires ATP for formation of a thioester adduct with ubiquitin. In principle, if E1 activity is impaired, protein ubiquitination should be diminished. To assess E1~Ub thioester levels, which are sensitive to reducing agents, the samples were run on SDS-PAGE under reducing (with β-mercaptoethanol) and non-reducing (without β-mercaptoethanol) conditions. As shown in Fig. 6A (*panel 1*), in the control sample under non-reducing conditions E1~Ub thioester (~126 kDa) migrated ~9 kDa above native E1 (117 kDa), consistent with the additional mass of ubiquitin. PGJ2 (15 μM) or $_{H}$IU1-treatment (50 μM) abolished the E1~Ub thioester, reflecting the loss of the ubiquitin monomer linked to E1 (Fig. 6A, panel 1). The effect of lower IU1 concentrations (≤ 25 μM) alone on E1~Ub thioester was minimal. As expected, when PGJ2 was combined with increasing concentrations of IU1 (Fig. 6A, panel 1), the E1~Ub thioester was almost undetectable. Under reducing conditions (Fig. 6A, panel 2) only native E1 was detected under all treatments.

We quantified the E1 protein levels (E1~Ub thioester + native E1) for all treatments (Fig. 6, bottom graphs on the right, n=3). IU1 (5 μM to 50 μM) did not alter E1 protein levels detected in control or PGJ2-treated neurons (*p values shown for each condition*), except when 50 μM was combined with PGJ2, which significantly reduced E1 protein levels (*p=0.0003*).

Moreover, 50 μM IU1 alone reduced E1~Ub thioester levels without affecting basal Ub-protein levels (Fig. 6A, panel 3, n=4, p>0.3, all conditions with IU1 alone compared to control). IU1 (5 μM to 25 μM) did not alter the accumulation of Ub-proteins induced by PGJ2 (*panel 3, n=4, p>0.6, PGJ2 compared with IU1+PGJ2).* In contrast, 50 μM IU1 induced a major down-regulation of Ub-proteins in PGJ2-treated neurons (*panel 3, n=4, p=0.0001, PGJ2 compared with PGJ2+IU1*). This reduction in Ub-proteins can be explained by the decrease in E1~Ub thioester and E1 protein levels (*panels 1 and 2*). Together, these data support that in neurons $_{H}$IU1-mediated ATP depletion correlates with lower E1~Ub thioester levels and under extreme conditions, loss of E1 levels. Unconjugated (free) ubiquitin and actin levels (Fig. 6A, panels 3 and 4, respectively) were not decreased by IU1.

3.5. PGJ2 induces a time-dependent decline in E1~Ub thioester formation while raising the levels of Ub-proteins in neurons. PGJ2 does not affect E1 and USP14 activities in vitro

We characterized the temporal effect of PGJ2 on E1~Ub thioester formation and compared it with the accumulation of Ub-proteins in the rat neurons. As shown in Fig. 6B (*panel 1*), 15 μM PGJ2 prevented E1~Ub thioester formation by 8 h of treatment. Moreover, PGJ2

increased the accumulation of Ub-proteins by 8 h of incubation (Fig. 6B, panel 3), despite the absence of E1~Ub thioester formation (Fig. 6B, panel 1). This seemingly paradoxical result is addressed in the discussion below.

Using a biochemically-defined assay for E1 thioester formation, we determined that PGJ2 did not directly inhibit E1 activity. As shown in Figure 6C, human E1~Ub was relatively stable for up to 24 hours in the presence of DMSO alone (*top panel*) or in the presence of 15 μM PGJ2 in DMSO (*bottom panel*).

We purified proteasomes associated with USP14 from wild type mouse brain extracts. To assess USP14 enzymatic activity in the absence or presence of increasing PGJ2 concentrations (10 μM to 100 μM), we used the HA-tagged Ub-derived active-site probe HA-Ub-VME to label the catalytically active DUB. As shown in Fig. 6D, PGJ2 did not affect the ubiquitin hydrolase activity of USP14 assessed by labeling of active USP 14 with the HA-Ub-VME probe.

3.6. $_{H}$IU1 induces a decline in 26S proteasomes and a concomitant increase in 20S proteasomes

The activity and assembly/disassembly of 26S proteasomes are highly dependent on ATP binding and hydrolysis [19,48]. We thus assessed with the native in-gel assay, the effects of IU1 on proteasome activity and levels in the cortical neurons. The in-gel assay detects the three assembled forms of the proteasome: 26S proteasomes with either two regulatory caps [26S(2)] or one cap [26S(1)], and the 20S core particle alone (20S). Proteasome activity was determined with the substrate Suc-LLVY-AMC, which assesses the chymotrypsin-like activity (Fig. 7). Under control conditions (*lanes marked with "0"*), the activity of the 20S proteasome is substantially lower than that of the 26S, because the 20S is a latent proteasome form [27]. Proteasome levels were determined by immunoblotting with the anti-Rpt6 antibody that reacts with an ATPase subunit of the 19S particle (Fig. 7, panel 3), and with the anti-β5 antibody (Fig. 7, panel 4). The β5 subunit is a component of the 20S core, thus its antibody detects assembled 26S and 20S proteasomes. It is clear that $_{H}$IU1 induced a decline in 26S proteasome activity that correlates with lower ATP levels [*compare* Fig 4A for ATP with Fig. 7 (panel 1) *for 26S proteasome activity*]. Furthermore, $_{H}$IU1 blocked 26S assembly (or promoted disassembly), as its activity and levels decreased while those of the 20S proteasome increased (Fig. 7, panels 1 and 2 for activity and panels 3 and 4 for levels). PGJ2-mediated inhibition of the 26S proteasome is shown for comparison. Semi-quantification of proteasome activity and levels for each condition is shown in Fig. 7B.

3.7. USP14 knockdown by siRNA or USP14 loss (Usp14^{axJ} mouse) failed to prevent the deleterious effects of PGJ2

To determine if lowering USP14 levels counteracts some of the PGJ2 effects observed in neurons, we induced USP14 knock down by siRNA prior to treatment with vehicle (control) or PGJ2 (Fig. 8B, panel 1). USP14 siRNA had no clear impact on the PGJ2-induced changes on neuronal viability (Fig. 8A), ΔTau, the caspase-dependent Tau fragment (Fig. 8B, panel 2), activated caspase 3 (Fig. 8B, panel 3), or ubiquitinated proteins (Fig. 8B, panel 4).

Likewise, studies with cortical cultures from *Usp14*^{axJ} mice [84] which exhibit a 90–95% loss of USP14 (Fig 9, panel 1), show that USP14 depletion failed to prevent the deleterious effects of PGJ2 tested, i.e. caspase-activation and accumulation of Ub-proteins (Fig. 9, panels 2 and 3, respectively).

4. Discussion

In this study we characterize the mechanism(s) by which the USP14 inhibitor IU1 affects the ubiquitin/proteasome pathway (UPP) in rat and mouse cerebral cortical neurons. In non-neuronal cells, IU1 is proposed to enhance the degradation of a range of proteasome substrates including Tau and oxidized proteins [44], which are implicated in neurodegenerative disorders such as AD, as well as misfolded prion proteins (PrP^{Sc}) relevant to prion diseases [54]. Thus, it was critical to investigate the impact of IU1 on neurons.

We show that IU1 concentrations >25 μM diminish the accumulation of Ub-proteins induced by PGJ2 in neurons, while IU1 concentrations ≤ 25 μM have no significant impact on Ub-protein levels. IU1 (75 μM) was previously shown to reduce menadione-induced accumulation of oxidized proteins in non-neuronal HEK293 cells [44]. Like PGJ2 [46,50], the vitamin K analog menadione (K3) induces accumulation of Ub-proteins [83,85]. However, whether or not IU1 blocks menadione-induced accumulation of Ub-proteins was not addressed [44]. This is important, as non-aggregated Ub-proteins are turned over by the 26S proteasome, the activity of which is potentially enhanced by inhibiting USP14 with IU1 [44]. On the other hand, most (70% to 80%) of all oxidized proteins that are not aggregated are degraded by 20S proteasomes in concert with immunoproteasomes [64]. The two latter forms of the proteasome do not associate with USP14 and are not postulated to be affected by IU1 [44,63]. We discuss below the impact of IU1 on 20S proteasome activity in neurons.

We also demonstrate that 75 μM IU1 induces calpain-dependent cleavage of endogenous Tau, as Tau cleavage is blocked by a calpain inhibitor (calpeptin). This is further supported by the finding that IU1-treatment clearly induces cleavage of α-spectrin (280 kDa) to 145/150 kDa fragments, which are indicative of calpain activation [81]. Moreover, the IU1-induced Tau fragments include a typical “17 kDa” fragment, which represents a marker for enhanced calpain activity in AD [21,25]. It is thus clear that IU1-induced Tau cleavage is mediated by calpain. We also established that the 26S proteasome activity is inhibited by 50 μM IU1.

Calpain-activation is linked to ATP-depletion and necrosis, a cell death pathway characterized by a bioenergetic crisis [86]. It is well established that calpain-activation is induced by mitochondrial inhibitors, such as oligomycin and antimycin [73]. Of relevance, we find that the pattern of IU1-induced Tau cleavage in neurons resembles that observed in our previous studies with these inhibitors [35]. In a similar manner, IU1 induced calpain-mediated cleavage of caspase 3 to a fragment (29 kDa) associated with caspase inactivation [35,61]. Calpain processing of caspase 3 to the 29 kDa inactive form could be a strategy to prevent execution of the apoptotic pathway under conditions of ATP-deficit, as apoptosis is an energy-dependent death pathway [86]. Together these data clearly show that IU1 (75 μM)

treatment in neurons activates calpain-dependent cleavage of Tau, spectrin and caspase 3, and suggest that IU1 may be neurotoxic and diminish intracellular ATP levels.

We established that IU1 is significantly neurotoxic even at low IU1 concentrations ($_{L}$IU1 ≤25 μM). Moreover, $_{H}$IU1-treatment stimulated calpain-dependent cleavage of a range of substrates, including Tau. These findings suggest that $_{H}$IU1-treatment induces cell death via necrosis and not apoptosis, since it induces calpain and not caspase 3 activation. Furthermore, $_{H}$IU1 concentrations (≥ 25 μM, in this case) cause mitochondrial dysfunction reflected in significant decreases in intracellular ATP levels. Of relevance, we show that IU1 inhibits mitochondrial Complex I *in vitro*. Taking into account the high degree of flux control of mitochondrial Complex I over oxidative phosphorylation in neuronal tissues [26,36,43], inhibition of even a small fraction of the enzyme, may lead to a significant decrease in ATP production by mitochondria [80] and decrease proteasomal activity [4,31,72]. It cannot be excluded that IU1 inhibition of NADH oxidation results in a change of redox state of the mitochondrial matrix leading to an imbalance of ROS metabolism. PGJ2-treatment combined with IU1 exacerbated the detrimental effects of IU1 on neuronal viability and ATP-level.

We demonstrate that IU1-treatment ($_{H}$IU1 >25 μM) impairs E1 and 26S proteasome activities, both of which are ATP-dependent [19,48,70,77]. $_{H}$IU1 hinders the ubiquitination cascade by blocking its first step; i.e., $_{H}$IU1 prevents ubiquitin-activation by the E1 enzyme, without decreasing free Ub levels. The combined treatment with PGJ2 and IU1 exacerbated the loss of E1 activity and level, compared to IU1 alone. Although IU1 alone has no apparent effect on basal Ub-protein levels, our data strongly support that IU1 prevents PGJ2-induced accumulation of Ub-proteins by blocking the ubiquitination cascade causing lower levels of Ub-proteins to be formed. IU1 does not enhance Ub-protein turnover by the 26S proteasome. This would explain why proteasome substrates such as TDP-43 accumulate as ubiquitinated-TDP-43 reflecting 26S proteasome inhibition (as discussed below), while little change was detected in bulk ubiquitin conjugates in IU1-treated non-neuronal cells [44].

$_{H}$IU1 elicited the demise of the 26S proteasome in neurons by diminishing its assembly, which partially correlates with ATP-depletion. Concomitant with the decline in 26S proteasomes, $_{H}$IU1-treatment induced a rise in 20S proteasome activity. Thus $_{H}$IU1 mimicked the effects of mitochondrial inhibitors on proteasomal function, as well as on calpain-activation and ATP-depletion [35]. We speculate that the significant increase in 20S proteasome activity induced by $_{H}$IU1-treatment, contributes to the reduction in menadione-induced accumulation of oxidized proteins in HEK293 cells [44]. Menadione is a highly toxic oxidant that elevates superoxide levels [23]. Upon ATP-depletion triggered by IU1-treatment it is possible that 20S proteasomes are recruited to promote turnover of oxidized proteins independently of ubiquitination [28,39]. Moreover, the 26S proteasome and the ubiquitination machinery are more vulnerable to oxidative damage than 20S proteasomes [65]. Autophagy is not likely to be involved in the degradation of menadione-induced oxidized proteins, as IU1 was shown to have no effect on autophagy [32].

As shown in the current studies, lowering USP14 levels by siRNA or 90% loss of USP14 exhibited by neuronal cultures from *Usp14*^{axJ} mice, failed to prevent or exacerbate the

detrimental effects of PGJ2 on caspase 3-activation and accumulation of Ub-proteins. These results are in agreement with studies with HeLa cells showing that siRNA for USP14 alone had no effect on cell growth, or the degradation of α-synuclein in U2OS cells or Tau in SH-SY5Y cells [41,42,62]. The combined siRNA approach to knockdown USP14 and another DUB UCH37, was necessary to observe accumulation of Ub-proteins [41,42]. The functional relationship among multiple deubiquitinases in terms of substrate hydrolysis and protein homeostasis in particular in neurons, requires further investigation.

Finally, we confirm that PGJ2 alone induces the accumulation of Ub-proteins. This is consistent with previous studies showing that PGJ2 lowers 26S proteasome levels and activity [37,55], and inhibits some of the thiol deubiquitinases including UCH-L1 and UCH-L3 [46,49], as well as Ub-isopeptidase activity [57], but not USP14 as shown here in our current studies. We also show for the first time, that PGJ2 lowers E1~Ub thioester levels. This result is surprising since we have shown that drugs that lower E1~Ub thioester levels, such as IU1 (current study) and mitochondrial inhibitors (oligomycin, antimycin and rotenone in [35]), do not cause accumulation of Ub-proteins in neurons. It is likely that the accumulation of Ub-proteins detected in PGJ2-treated neurons reflects its ability to inhibit some deubiquitinases thereby leading to the stabilization of Ub-proteins formed prior to E1~Ub thioester depletion.

In conclusion, our findings strongly support that pharmacologically inhibiting (with low or high IU1 concentrations) or genetically down-regulating USP14 fail to enhance proteasomal degradation of Ub-proteins in neurons. Studies by others show a similar trend. A recent study with mice reported that the catalytic activity of USP14 is necessary for nervous system structure and function and has an ongoing role in neuromuscular junction synaptic transmission [79]. Another study demonstrated that siRNA for USP14 alone has no effect on the degradation of α-synuclein in U2OS cells or Tau in SH-SY5Y cells [62].

IU1 seems to have off-target effects, such as inhibiting mitochondrial Complex 1 that is damaging to neurons. It is conceivable that data obtained with non-neuronal cells may not always be directly comparable in neurons, in particular because the pharmacodynamics in neurons may be more sensitive and/or have mechanisms that are not replicated in non-neuronal cells. We established that neurons accumulate IU1 to a higher intracellular concentration than that previously reported in MEFs [44]. Using mass spectrometry we determined that neurons accumulate IU1 to ~90% of the extracellular concentration, while MEFs were determined to accumulate IU1 to only 26% of the extracellular concentration [44]. The reason for this discrepancy remains to be established, but it may explain why neurons are more sensitive to IU1 toxicity than MEFs.

Our data do not exclude the possibility that inhibiting USP14 (aside from IU1) is beneficial against certain conditions that disturb protein homeostasis. For example, inhibiting USP14 with three specific RNA aptamers (single-stranded synthetic RNA molecules that act like “chemical antibodies” [20]) facilitated the degradation of Tau conditionally expressed in HeLa cells [45]. However, our data clearly show that in neurons, IU1-induced cleavage of endogenous Tau is mediated by calpain and not by proteasomal-dependent degradation, as 26S proteasome activity was inhibited by IU1-treatment.

Due to the deleterious effects of IU1 on neurons and to the magnitude and diversity of the enzymes involved in the UPP, a detailed understanding of their relationships in neurons is of the utmost therapeutic interest, since reducing the abnormal levels of Ub-proteins in neurons is highly relevant to neurodegenerative disorders, such as AD and PD [34].

Acknowledgments

We thank Dr. P. Rockwell (Hunter College, CUNY) for insightful discussions and Dr. L. Binder (Northwestern University, Chicago, IL) for the Tau C3 ad Tau C5 antibodies. This work was supported by NIH [U54 NS041073 (SNRP, expired) to M.E.F.-P head of sub-project from NINDS, and NCRR-RR003037 (infrastructure) to Hunter College, City University of New York from NIGMS/RCMI], MRC UK MR/L007339/1 to A.G., and the City University of New York (Ph.D. program in Biochemistry, Graduate Center).

Abbreviations

AD	Alzheimer disease
BCA	bicinchoninic acid
Clp	calpeptin, calpain inhibitor Z-Leu-Nle-CHO
DMEM	Dulbecco’s modified eagle’s medium
DMSO	dimethyl sulfoxide
DTT	dithiothreitol
ECL	enhanced chemiluminescence
HAR	hexaammineruthenium
HA-Ub-VME	hemagglutinin-tagged ubiquitin vinyl methyl ester
IU1	1-[1-(4-Fluoro-phenyl)-2,5-dimethyl-1H-pyrrol-3-yl]-2-pyrrolidin-1-yl-ethanone
MTT	3-(4,5-dimethylthiazol-2-yl)-2,5-diphenyl tetrazolium bromide
PAGE	polyacrylamide gel electrophoresis
PBS	phosphate buffer saline
PGJ2	prostaglandin J2
Q_1	2,3-dimethoxy-5-methyl-6-(3-methyl-2-butenyl)-1,4-benzoquinone
ROS	reactive oxygen species
Rpn	regulatory particle non-ATPase
Rpt	regulatory particle triple-A ATPase
SDS	sodium dodecyl sulfate

SMPs	submitochondrial particles
Suc-LLVY-AMC	succinyl-Leu-Leu-Val-Tyr-7-amino-4-methylcoumarin
Tau FL	full length Tau
Δ Tau	Tau cleaved at Asp421
Ub-protein	ubiquitin conjugate
UPP	ubiquitin/proteasome pathway
USP14	ubiquitin specific peptidase 14

References

1. Anderson C, Crimmins S, Wilson JA, Korbel GA, Ploegh HL, Wilson SM. Loss of Usp14 results in reduced levels of ubiquitin in ataxia mice. J Neurochem. 2005; 95:724–731. [PubMed: 16190881]
2. Arnaud LT, Myeku N, Figueiredo-Pereira ME. Proteasome-caspase-cathepsin sequence leading to tau pathology induced by prostaglandin J2 in neuronal cells. J Neurochem. 2009; 110:328–342. [PubMed: 19457109]
3. Baboshina OV, Haas AL. Novel multiubiquitin chain linkages catalyzed by the conjugating enzymes E2EPF and RAD6 are recognized by 26 S proteasome subunit 5. J Biol Chem. 1996; 271:2823–2831. [PubMed: 8576261]
4. Benaroudj N, Zwickl P, Seemuller E, Baumeister W, Goldberg AL. ATP hydrolysis by the proteasome regulatory complex PAN serves multiple functions in protein degradation. Mol Cell. 2003; 11:69–78. [PubMed: 12535522]
5. Berridge MV, Tan AS. Characterization of the cellular reduction of 3-(4,5-dimethylthiazol-2-yl)-2,5-diphenyltetrazolium bromide (MTT): subcellular localization, substrate dependence, and involvement of mitochondrial electron transport in MTT reduction. Arch Biochem Biophys. 1993; 303:474–482. [PubMed: 8390225]
6. Borodovsky A, Kessler BM, Casagrande R, Overkleeft HS, Wilkinson KD, Ploegh HL. A novel active site-directed probe specific for deubiquitylating enzymes reveals proteasome association of USP14. EMBO J. 2001; 20:5187–5196. [PubMed: 11566882]
7. Borodovsky A, Ovaa H, Kolli N, Gan-Erdene T, Wilkinson KD, Ploegh HL, Kessler BM. Chemistry-based functional proteomics reveals novel members of the deubiquitinating enzyme family. Chem Biol. 2002; 9:1149–1159. [PubMed: 12401499]
8. Brewer GJ, Torricelli JR, Evege EK, Price PJ. Optimized survival of hippocampal neurons in B27-supplemented Neurobasal, a new serum-free medium combination. J Neurosci Res. 1993; 35:567–576. [PubMed: 8377226]
9. Chen PC, Bhattacharyya BJ, Hanna J, Minkel H, Wilson JA, Finley D, Miller RJ, Wilson SM. Ubiquitin homeostasis is critical for synaptic development and function. J Neurosci. 2011; 31:17505–17513. [PubMed: 22131412]
10. Chinopoulos C, Zhang SF, Thomas B, Ten V, Starkov AA. Isolation and functional assessment of mitochondria from small amounts of mouse brain tissue. Methods Mol Biol. 2011; 793:311–324. [PubMed: 21913109]
11. Clague MJ, Barsukov I, Coulson JM, Liu H, Rigden DJ, Urbe S. Deubiquitylases from genes to organism. Physiol Rev. 2013; 93:1289–1315. [PubMed: 23899565]
12. Crimmins S, Sutovsky M, Chen PC, Huffman A, Wheeler C, Swing DA, Roth K, Wilson J, Sutovsky P, Wilson S. Transgenic rescue of ataxia mice reveals a male-specific sterility defect. Dev Biol. 2009; 325:33–42. [PubMed: 18926813]
13. Crosas B. Deubiquitinating enzyme inhibitors and their potential in cancer therapy. Curr Cancer Drug Targets. 2014; 14:506–516. [PubMed: 25088039]

14. D'Amato CJ, Hicks SP. Neuropathologic alterations in the ataxia (paralytic) mouse. Arch Pathol. 1965; 80:604–612. [PubMed: 5855800]
15. Day JJ, Childs D, Guzman-Karlsson MC, Kibe M, Moulden J, Song E, Tahir A, Sweatt JD. DNA methylation regulates associative reward learning. Nat Neurosci. 2013; 16:1445–1452. [PubMed: 23974711]
16. de Calignon A, Fox LM, Pitstick R, Carlson GA, Bacskai BJ, Spires-Jones TL, Hyman BT. Caspase activation precedes and leads to tangles. Nature. 2010; 464:1201–1204. [PubMed: 20357768]
17. Edelmann MJ, Nicholson B, Kessler BM. Pharmacological targets in the ubiquitin system offer new ways of treating cancer, neurodegenerative disorders and infectious diseases. Expert Rev Mol Med. 2011; 13:e35. [PubMed: 22088887]
18. Eletr ZM, Wilkinson KD. Regulation of proteolysis by human deubiquitinating enzymes. Biochim Biophys Acta. 2014; 1843:114–128. [PubMed: 23845989]
19. Eytan E, Ganoth D, Armon T, Hershko A. ATP-dependent incorporation of 20S protease into the 26S complex that degrades proteins conjugated to ubiquitin. Proc Natl Acad Sci U S A. 1989; 86:7751–7755. [PubMed: 2554287]
20. Famulok M, Mayer G, Blind M. Nucleic acid aptamers-from selection in vitro to applications in vivo. Acc Chem Res. 2000; 33:591–599. [PubMed: 10995196]
21. Ferreira A, Bigio EH. Calpain-mediated tau cleavage: a mechanism leading to neurodegeneration shared by multiple tauopathies. Mol Med. 2011; 17:676–685. [PubMed: 21442128]
22. Figueiredo-Pereira ME, Rockwell P, Schmidt-Glenewinkel T, Serrano P. Neuroinflammation and J2 prostaglandins: linking impairment of the ubiquitin-proteasome pathway and mitochondria to neurodegeneration. Frontiers in Mol Neurosci. 2015; 7:104.
23. Fukui M, Choi HJ, Zhu BT. Rapid generation of mitochondrial superoxide induces mitochondrion-dependent but caspase-independent cell death in hippocampal neuronal cells that morphologically resembles necroptosis. Toxicol Appl Pharmacol. 2012; 262:156–166. [PubMed: 22575170]
24. Gamblin TC, Chen F, Zambrano A, Abraha A, Lagalwar S, Guillozet AL, Lu M, Fu Y, Garcia-Sierra F, LaPointe N, Miller R, Berry RW, Binder LI, Cryns VL. Caspase cleavage of tau: linking amyloid and neurofibrillary tangles in Alzheimer's disease. Proc Natl Acad Sci U S A. 2003; 100:10032–10037. [PubMed: 12888622]
25. Garg S, Timm T, Mandelkow EM, Mandelkow E, Wang Y. Cleavage of Tau by calpain in Alzheimer's disease: the quest for the toxic 17 kD fragment. Neurobiol Aging. 2011; 32:1–14. [PubMed: 20961659]
26. Genova ML, Castelluccio C, Fato R, Parenti CG, Merlo PM, Formiggini G, Bovina C, Marchetti M, Lenaz G. Major changes in complex I activity in mitochondria from aged rats may not be detected by direct assay of NADH:coenzyme Q reductase. Biochem J. 1995; 311(Pt 1):105–109. [PubMed: 7575440]
27. Goldberg AL. Functions of the proteasome: from protein degradation and immune surveillance to cancer therapy. Biochem Soc Trans. 2007; 35:12–17. [PubMed: 17212580]
28. Grune T, Jung T, Merker K, Davies KJ. Decreased proteolysis caused by protein aggregates, inclusion bodies, plaques, lipofuscin, ceroid, and 'aggresomes' during oxidative stress, aging, and disease. Int J Biochem Cell Biol. 2004; 36:2519–2530. [PubMed: 15325589]
29. Haas AL. Purification of E1 and E1-like enzymes. Methods Mol Biol. 2005; 301:23–35. [PubMed: 15917623]
30. Hertting G, Seregi A. Formation and function of eicosanoids in the central nervous system. Ann N Y Acad Sci. 1989; 559:84–99. [PubMed: 2672946]
31. Hoglinger GU, Carrard G, Michel PP, Medja F, Lombes A, Ruberg M, Friguet B, Hirsch EC. Dysfunction of mitochondrial complex I and the proteasome: interactions between two biochemical deficits in a cellular model of Parkinson's disease. J Neurochem. 2003; 86:1297–1307. [PubMed: 12911637]
32. Homma T, Ishibashi D, Nakagaki T, Fuse T, Mori T, Satoh K, Atarashi R, Nishida N. Ubiquitin-specific protease 14 modulates degradation of cellular prion protein. Sci Rep. 2015; 5:11028. [PubMed: 26061634]

33. Hu M, Li P, Song L, Jeffrey PD, Chenova TA, Wilkinson KD, Cohen RE, Shi Y. Structure and mechanisms of the proteasome-associated deubiquitinating enzyme USP14. EMBO J. 2005; 24:3747–3756. [PubMed: 16211010]

34. Huang Q, Figueiredo-Pereira ME. Ubiquitin/proteasome pathway impairment in neurodegeneration: therapeutic implications. Apoptosis. 2010; 15:1292–1311. [PubMed: 20131003]

35. Huang Q, Wang H, Perry SW, Figueiredo-Pereira ME. Negative regulation of 26S proteasome stability via calpain-mediated cleavage of Rpn10 subunit upon mitochondrial dysfunction in neurons. J Biol Chem. 2013; 288:12161–12174. [PubMed: 23508964]

36. Inomoto T, Tanaka A, Mori S, Jin MB, Sato B, Yanabu N, Tokuka A, Kitai T, Ozawa K, Yamaoka Y. Changes in the distribution of the control of the mitochondrial oxidative phosphorylation in regenerating rabbit liver. Biochim Biophys Acta. 1994; 1188:311–317. [PubMed: 7803448]

37. Ishii T, Sakurai T, Usami H, Uchida K. Oxidative modification of proteasome: identification of an oxidation-sensitive subunit in 26 s proteasome. Biochemistry. 2005; 44:13893–13901. [PubMed: 16229478]

38. Jha N, Kumar MJ, Boonplueang R, Andersen JK. Glutathione decreases in dopaminergic PC12 cells interfere with the ubiquitin protein degradation pathway: relevance for Parkinson's disease? J Neurochem. 2002; 80:555–561. [PubMed: 11841562]

39. Kastle M, Grune T. Proteins bearing oxidation-induced carbonyl groups are not preferentially ubiquitinated. Biochimie. 2011; 93:1076–1079. [PubMed: 21402121]

40. Koharudin LM, Liu H, Di MR, Kodali RB, Graham SH, Gronenborn AM. Cyclopentenone prostaglandin-induced unfolding and aggregation of the Parkinson disease-associated UCH-L1. Proc Natl Acad Sci U S A. 2010; 107:6835–6840. [PubMed: 20231490]

41. Komander D, Clague MJ, Urbe S. Breaking the chains: structure and function of the deubiquitinases. Nat Rev Mol Cell Biol. 2009; 10:550–563. [PubMed: 19626045]

42. Koulich E, Li X, DeMartino GN. Relative structural and functional roles of multiple deubiquitylating proteins associated with mammalian 26S proteasome. Mol Biol Cell. 2008; 19:1072–1082. [PubMed: 18162577]

43. Kuznetsov AV, Winkler K, Kirches E, Lins H, Feistner H, Kunz WS. Application of inhibitor titrations for the detection of oxidative phosphorylation defects in saponin-skinned muscle fibers of patients with mitochondrial diseases. Biochim Biophys Acta. 1997; 1360:142–150. [PubMed: 9128179]

44. Lee BH, Lee MJ, Park S, Oh DC, Elsasser S, Chen PC, Gartner C, Dimova N, Hanna J, Gygi SP, Wilson SM, King RW, Finley D. Enhancement of proteasome activity by a small-molecule inhibitor of USP14. Nature. 2010; 467:179–184. [PubMed: 20829789]

45. Lee JH, Shin SK, Jiang Y, Choi WH, Hong C, Kim DE, Lee MJ. Facilitated Tau Degradation by USP14 Aptamers via Enhanced Proteasome Activity. Sci Rep. 2015; 5:10757. [PubMed: 26041011]

46. Li Z, Melandri F, Berdo I, Jansen M, Hunter L, Wright S, Valbrun D, Figueiredo-Pereira ME. Δ12-Prostaglandin J2 inhibits the ubiquitin hydrolase UCH-L1 and elicits ubiquitin-protein aggregation without proteasome inhibition. Biochem Biophys Res Commun. 2004; 319:1171–1180. [PubMed: 15194490]

47. Liang X, Wu L, Hand T, Andreasson K. Prostaglandin D2 mediates neuronal protection via the DP1 receptor. J Neurochem. 2005; 92:477–486. [PubMed: 15659218]

48. Liu CW, Li X, Thompson D, Wooding K, Chang TL, Tang Z, Yu H, Thomas PJ, DeMartino GN. ATP binding and ATP hydrolysis play distinct roles in the function of 26S proteasome. Mol Cell. 2006; 24:39–50. [PubMed: 17018291]

49. Liu H, Li W, Ahmad M, Miller TM, Rose ME, Poloyac SM, Uechi G, Balasubramani M, Hickey RW, Graham SH. Modification of ubiquitin-C-terminal hydrolase-L1 by cyclopentenone prostaglandins exacerbates hypoxic injury. Neurobiol Dis. 2011; 41:318–328. [PubMed: 20933087]

50. Liu H, Li W, Ahmad M, Rose ME, Miller TM, Yu M, Chen J, Pascoe JL, Poloyac SM, Hickey RW, Graham SH. Increased generation of cyclopentenone prostaglandins after brain ischemia and their

role in aggregation of ubiquitinated proteins in neurons. Neurotox Res. 2013; 24:191–204. [PubMed: 23355003]

51. Liu H, Li W, Rose ME, Pascoe JL, Miller TM, Ahmad M, Poloyac SM, Hickey RW, Graham SH. Prostaglandin D toxicity in primary neurons is mediated through its bioactive cyclopentenone metabolites. Neurotoxicology. 2013; 39C:35–44.
52. Liu Y, Peterson DA, Kimura H, Schubert D. Mechanism of cellular 3-(4,5-dimethylthiazol-2-yl)-2,5-diphenyltetrazolium bromide (MTT) reduction. J Neurochem. 1997; 69:581–593. [PubMed: 9231715]
53. Mandelkow E, Von BM, Biernat J, Mandelkow EM. Structural principles of tau and the paired helical filaments of Alzheimer's disease. Brain Pathol. 2007; 17:83–90. [PubMed: 17493042]
54. McKinnon C, Goold R, Andre R, Devoy A, Ortega Z, Moonga J, Linehan JM, Brandner S, Lucas JJ, Collinge J, Tabrizi SJ. Prion-mediated neurodegeneration is associated with early impairment of the ubiquitin-proteasome system. Acta Neuropathol. 2016; 131:411–425. [PubMed: 26646779]
55. Metcalfe MJ, Huang Q, Figueiredo-Pereira ME. Coordination between proteasome impairment and caspase activation leading to TAU pathology: neuroprotection by cAMP. Cell Death Dis. 2012; 3:e326. [PubMed: 22717581]
56. Mosmann T. Rapid colorimetric assay for cellular growth and survival: application to proliferation and cytotoxicity assays. J Immunol Methods. 1983; 65:55–63. [PubMed: 6606682]
57. Mullally JE, Moos PJ, Edes K, Fitzpatrick FA. Cyclopentenone prostaglandins of the J series inhibit the ubiquitin isopeptidase activity of the proteasome pathway. J Biol Chem. 2001; 276:30366–30373. [PubMed: 11390388]
58. Myeku N, Metcalfe MJ, Huang Q, Figueiredo-Pereira M. Assessment of proteasome impairment and accumulation/aggregation of ubiquitinated proteins in neuronal cultures. Methods Mol Biol. 2011; 793:273–296. [PubMed: 21913107]
59. Nam Y, Brewer GJ, Wheeler BC. Development of astroglial cells in patterned neuronal cultures. J Biomater Sci Polym Ed. 2007; 18:1091–1100. [PubMed: 17706000]
60. Ogburn KD, Figueiredo-Pereira ME. Cytoskeleton/endoplasmic reticulum collapse induced by prostaglandin J2 parallels centrosomal deposition of ubiquitinated protein aggregates. J Biol Chem. 2006; 281:23274–23284. [PubMed: 16774923]
61. Orrenius S, Zhivotovsky B, Nicotera P. Regulation of cell death: the calcium-apoptosis link. Nat Rev Mol Cell Biol. 2003; 4:552–565. [PubMed: 12838338]
62. Ortuno D, Carlisle HJ, Miller S. Does inactivation of USP14 enhance degradation of proteasomal substrates that are associated with neurodegenerative diseases? F1000Res. 2016; 5:137. [PubMed: 26998235]
63. Peth A, Besche HC, Goldberg AL. Ubiquitinated proteins activate the proteasome by binding to Usp14/Ubp6, which causes 20S gate opening. Mol Cell. 2009; 36:794–804. [PubMed: 20005843]
64. Pickering AM, Koop AL, Teoh CY, Ermak G, Grune T, Davies KJ. The immunoproteasome, the 20S proteasome and the PA28αβ proteasome regulator are oxidative-stress-adaptive proteolytic complexes. Biochem J. 2010; 432:585–594. [PubMed: 20919990]
65. Reinheckel T, Sitte N, Ullrich O, Kuckelkorn U, Davies KJ, Grune T. Comparative resistance of the 20S and 26S proteasome to oxidative stress. Biochem J. 1998; 335(Pt 3):637–642. [PubMed: 9794805]
66. Rissman RA, Poon WW, Blurton-Jones M, Oddo S, Torp R, Vitek MP, LaFerla FM, Rohn TT, Cotman CW. Caspase-cleavage of tau is an early event in Alzheimer disease tangle pathology. J Clin Invest. 2004; 114:121–130. [PubMed: 15232619]
67. Ristic G, Tsou WL, Todi SV. An optimal ubiquitin-proteasome pathway in the nervous system: the role of deubiquitinating enzymes. Front Mol Neurosci. 2014; 7:72. [PubMed: 25191222]
68. Rungta RL, Choi HB, Lin PJ, Ko RW, Ashby D, Nair J, Manoharan M, Cullis PR, Macvicar BA. Lipid nanoparticle delivery of siRNA to silence neuronal gene expression in the brain. Mol Ther Nucleic Acids. 2013; 2:e136. [PubMed: 24301867]
69. Satoh T, Lipton SA. Redox regulation of neuronal survival mediated by electrophilic compounds. Trends Neurosci. 2007; 30:37–45. [PubMed: 17137643]
70. Schulman BA, Harper JW. Ubiquitin-like protein activation by E1 enzymes: the apex for downstream signalling pathways. Nat Rev Mol Cell Biol. 2009; 10:319–331. [PubMed: 19352404]

71. Shaik JS, Miller TM, Graham SH, Manole MD, Poloyac SM. Rapid and simultaneous quantitation of prostanoids by UPLC-MS/MS in rat brain. J Chromatogr B Analyt Technol Biomed Life Sci. 2014; 945–946:207–216.
72. Shamoto-Nagai M, Maruyama W, Kato Y, Isobe K, Tanaka M, Naoi M, Osawa T. An inhibitor of mitochondrial complex I, rotenone, inactivates proteasome by oxidative modification and induces aggregation of oxidized proteins in SH-SY5Y cells. J Neurosci Res. 2003; 74:589–597. [PubMed: 14598303]
73. Shell JR, Lawrence DS. Proteolytic regulation of the mitochondrial cAMP-dependent protein kinase. Biochemistry. 2012; 51:2258–2264. [PubMed: 22385295]
74. Shibata T, Yamada T, Kondo M, Tanahashi N, Tanaka K, Nakamura H, Masutani H, Yodoi J, Uchida K. An endogenous electrophile that modulates the regulatory mechanism of protein turnover: inhibitory effects of 15-deoxy-Δ(12,14)-prostaglandin J2 on proteasome. Biochemistry. 2003; 42:13960–13968. [PubMed: 14636064]
75. Stepanova A, Shurubor Y, Valsecchi F, Manfredi G, Galkin A. Differential susceptibility of mitochondrial complex II to inhibition by oxaloacetate in brain and heart. Biochim Biophys Acta. 2016; 1857:1561–1568. [PubMed: 27287543]
76. Straus DS, Glass CK. Cyclopentenone prostaglandins: new insights on biological activities and cellular targets. Med Res Rev. 2001; 21:185–210. [PubMed: 11301410]
77. Tokgoz Z, Bohnsack RN, Haas AL. Pleiotropic effects of ATP•Mg^{2+} binding in the catalytic cycle of ubiquitin-activating enzyme. J Biol Chem. 2006; 281:14729–14737. [PubMed: 16595681]
78. Uchida K, Shibata T. 15-Deoxy-Δ(12,14)-prostaglandin J2: an electrophilic trigger of cellular responses. Chem Res Toxicol. 2008; 21:138–144. [PubMed: 18052108]
79. Vaden JH, Watson JA, Howard AD, Chen PC, Wilson JA, Wilson SM. Distinct effects of ubiquitin overexpression on NMJ structure and motor performance in mice expressing catalytically inactive USP14. Front Mol Neurosci. 2015; 8:11. [PubMed: 25954152]
80. Ventura B, Genova ML, Bovina C, Formiggini G, Lenaz G. Control of oxidative phosphorylation by Complex I in rat liver mitochondria: implications for aging. Biochim Biophys Acta. 2002; 1553:249–260. [PubMed: 11997134]
81. Wang KK. Calpain and caspase: can you tell the difference? Trends Neurosci. 2000; 23:20–26. [PubMed: 10631785]
82. Wang Z, Aris VM, Ogburn KD, Soteropoulos P, Figueiredo-Pereira ME. Prostaglandin J2 alters pro-survival and pro-death gene expression patterns and 26 S proteasome assembly in human neuroblastoma cells. J Biol Chem. 2006; 281:21377–21386. [PubMed: 16737963]
83. Wilkie-Grantham RP, Matsuzawa S, Reed JC. Novel phosphorylation and ubiquitination sites regulate reactive oxygen species-dependent degradation of anti-apoptotic c-FLIP protein. J Biol Chem. 2013; 288:12777–12790. [PubMed: 23519470]
84. Wilson SM, Bhattacharyya B, Rachel RA, Coppola V, Tessarollo L, Householder DB, Fletcher CF, Miller RJ, Copeland NG, Jenkins NA. Synaptic defects in ataxia mice result from a mutation in Usp14, encoding a ubiquitin-specific protease. Nat Genet. 2002; 32:420–425. [PubMed: 12368914]
85. Yu C, Huang X, Xu Y, Li H, Su J, Zhong J, Kang J, Liu Y, Sun L. Lysosome dysfunction enhances oxidative stress-induced apoptosis through ubiquitinated protein accumulation in Hela cells. Anat Rec (Hoboken). 2013; 296:31–39. [PubMed: 23125185]
86. Zong WX, Thompson CB. Necrotic death as a cell fate. Genes Dev. 2006; 20:1–15. [PubMed: 16391229]

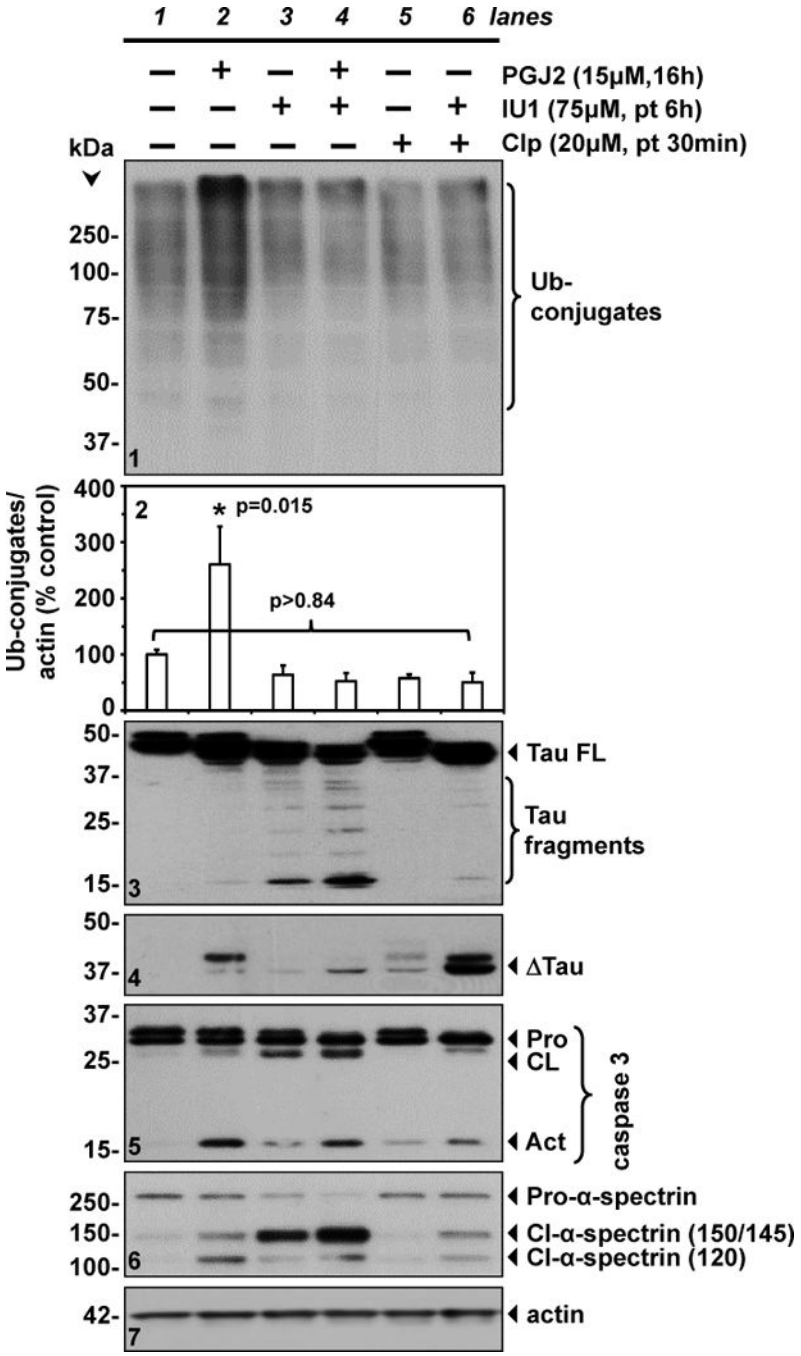

FIGURE 1. Effects of IU1, PGJ2 and calpeptin treatments (independently or combined) on rat cerebral cortical neurons

Neurons were treated with DMSO (vehicle, control, *lane 1*), PGJ2 (15 μM, *lane 2*), IU1 (75 μM, *lane 3*) or calpeptin (20 μM, Clp, calpain inhibitor, *lane 5*) independently. In addition, the following combinations were tested: IU1 + PGJ2 (*lane 4*), or calpeptin + IU1 (*lane 6*). IU1 was added 6 h prior to PGJ2, and Clp was added 30 min prior to IU1. Following pre-treatment neurons were incubated with DMSO or PGJ2 for an additional 16 h. Total lysates were analyzed by western blotting (30 μg of protein/lane) probed with the respective antibodies to detect: Ub-proteins (*panel 1*), Tau (*panels 3 and 4*), caspase 3 (*panel 5*), α-

spectrin (*panel 6*), or actin (loading control, *panel 7*). Molecular mass markers in kDa are shown on the left. Similar data were obtained in at least triplicate experiments. In panel 2 the levels of Ub-proteins (Ub-conjugates/actin) were semi-quantified by densitometry. Data represent the percentage of the pixel ratio for Ub-proteins over actin for each condition compared to control (100%). Values are means from four (n=4) independent experiments ± s.e. (standard error). The asterisk identifies the value that is significantly different from control (* $p = 0.015$); all other values are not significantly different from control ($p>0.84$). Pro (full length), Cl (cleaved) and Act (active) caspase 3; Tau FL, full length Tau; Δ Tau, caspase-dependent Tau cleaved at Asp421; pt, pre-treatment; Ub, ubiquitinated.

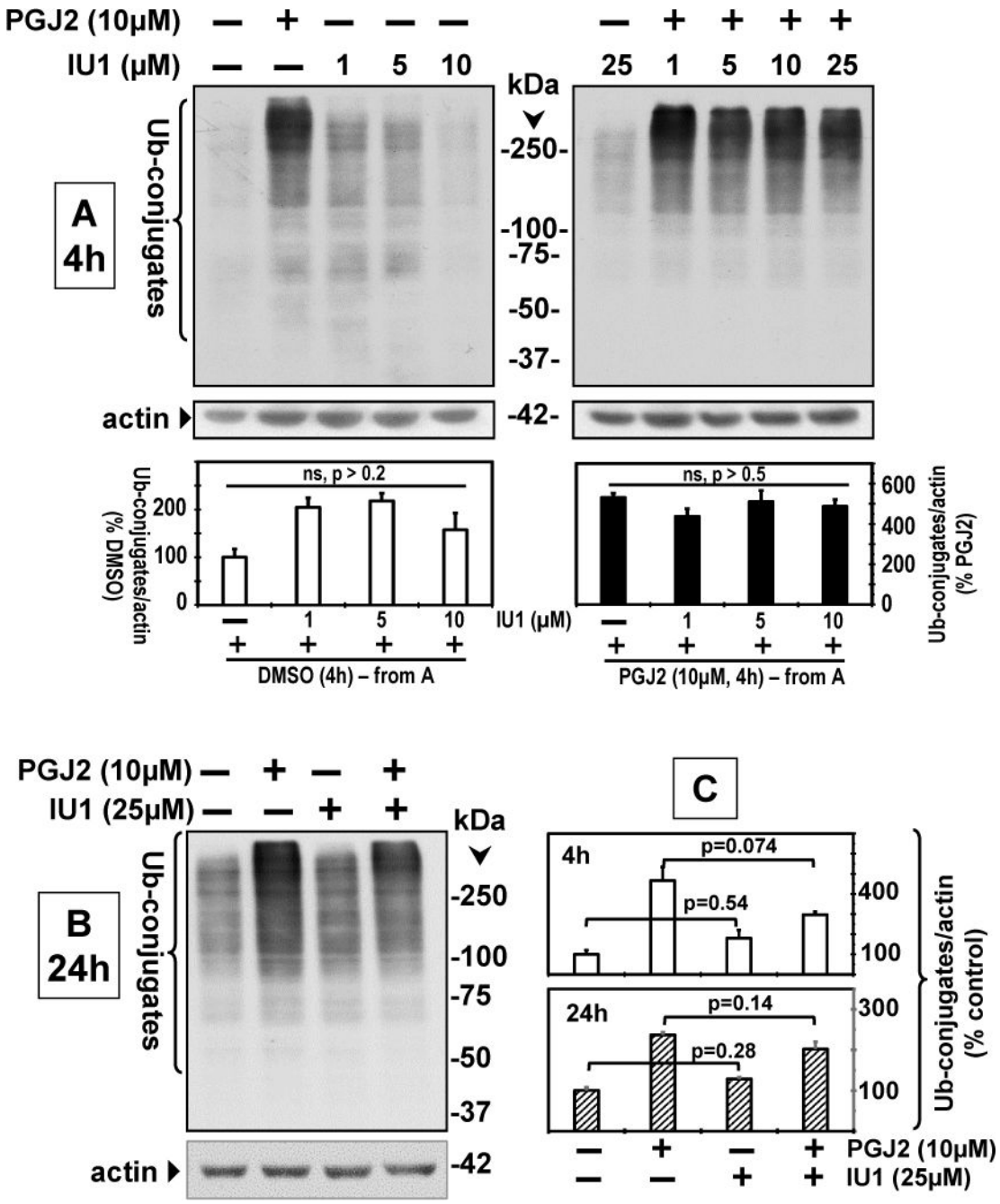

FIGURE 2. Effects of IU1 and PGJ2 treatments (alone or as co-treatment) on rat cerebral cortical neurons

Neurons were treated with DMSO (vehicle, control), PGJ2 alone (10 μM), different concentrations of IU1 (1 μM to 25 μM) alone or with PGJ2 for 4 h (A) or for 24 h with 25 μM IU1 alone or with PGJ2 (B). Total lysates were analyzed by western blotting (30 μg of protein/lane) probed with the respective antibodies to detect ubiquitinated (Ub)-proteins or actin (loading control). Molecular mass markers in kDa are shown in the center (4 h) or on the right (24 h). In (A) and (B, shown in C) the levels of Ub-proteins as Ub-proteins/actin ratios were semi-quantified by densitometry. Values are means from three (A, n=3) or four

(B, n=4) independent experiments ± s.e. (standard error). Data represent the percentage of the pixel ratio for Ub-proteins/actin for each condition compared to control (100%). In (A), all the *p* values determined by comparing Ub-protein levels in control or PGJ2-treated neurons with those when 1 μM, 5 μM, or 10 μM IU1 was added (n=4) were ≥0.2, thus non-significant. In (B, shown in C) the *p* values represent Ub-protein levels that are not significantly different (p>0.07).

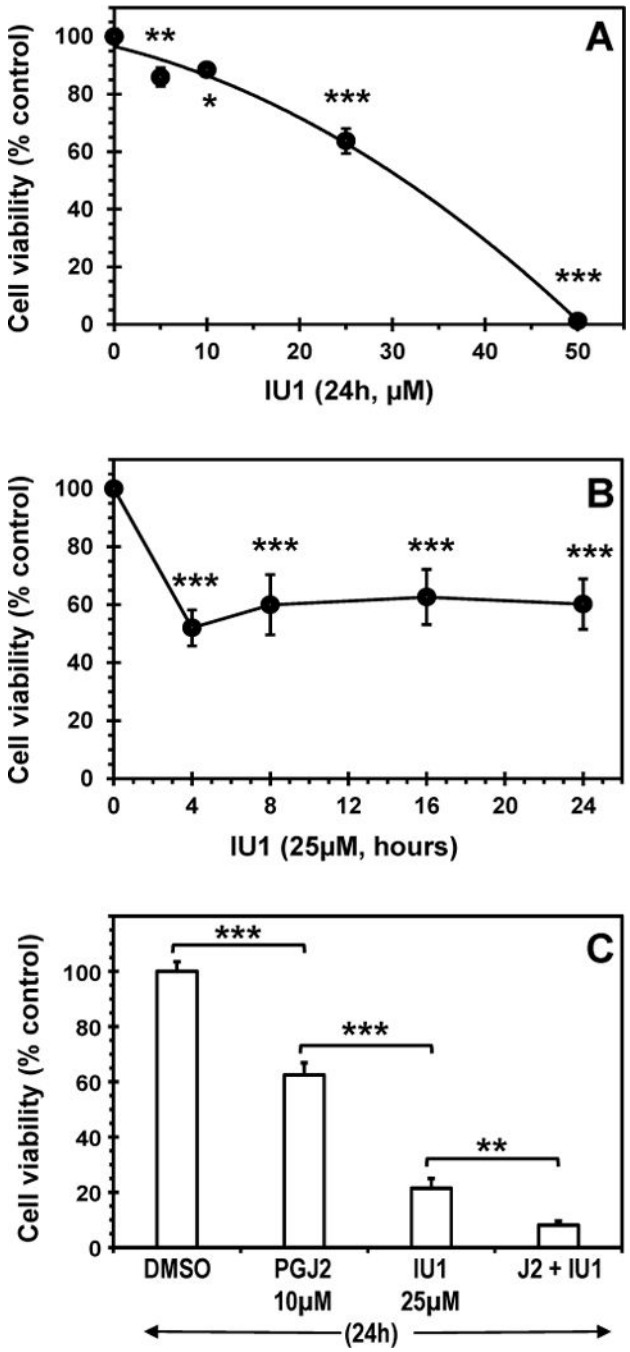

FIGURE 3. Effect of IU1 or/and PGJ2 on the viability of rat cerebral cortical neurons

Neurons were treated with increasing concentrations of IU1 (24 h, A), or with 25 μM IU1 for different times (B), or with IU1 (25 μM) or PGJ2 (10 μM) alone or as a co-treatment for 24 h (C). Neuronal viability was assessed with the MTT assay. Percentages represent the ratio between the data for each condition and control (100%). Values indicate means and s.e. from at least three independent experiments per group. Asterisks identify values that are significantly different from control (* $p<0.05$; ** $p<0.01$; *** $p<0.001$).

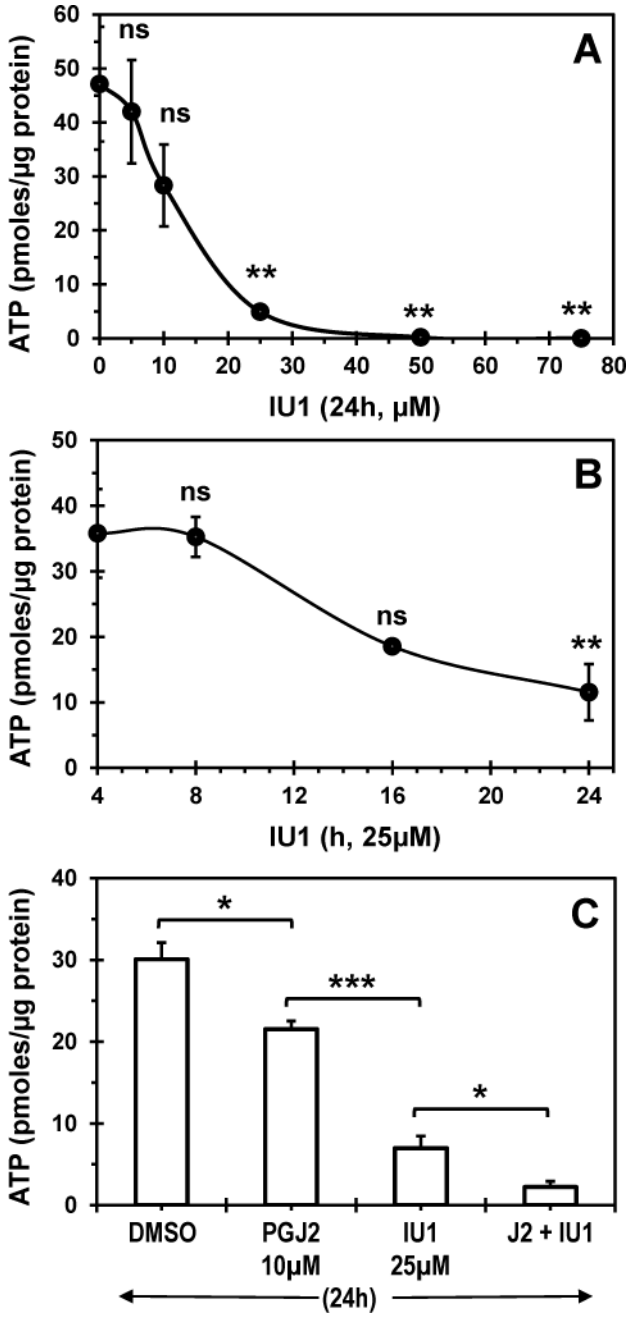

FIGURE 4. Effect of IU1 or/and PGJ2 on ATP levels in rat cerebral cortical neurons

Neurons were treated with increasing concentrations of IU1 (24 h, A), or with 25 µM IU1 for different times (B), or with IU1 (25 µM) or PGJ2 (10 µM) alone or as a co-treatment for 24 h (C). ATP steady state levels (pmoles/µg of protein) were assessed with the luciferin/luciferase system. Values indicate means and s.e. from at least three independent experiments per group. Asterisks identify values that are significantly different from control (* $p<0.05$; ** $p<0.01$; *** $p<0.001$); ns, not significantly different.

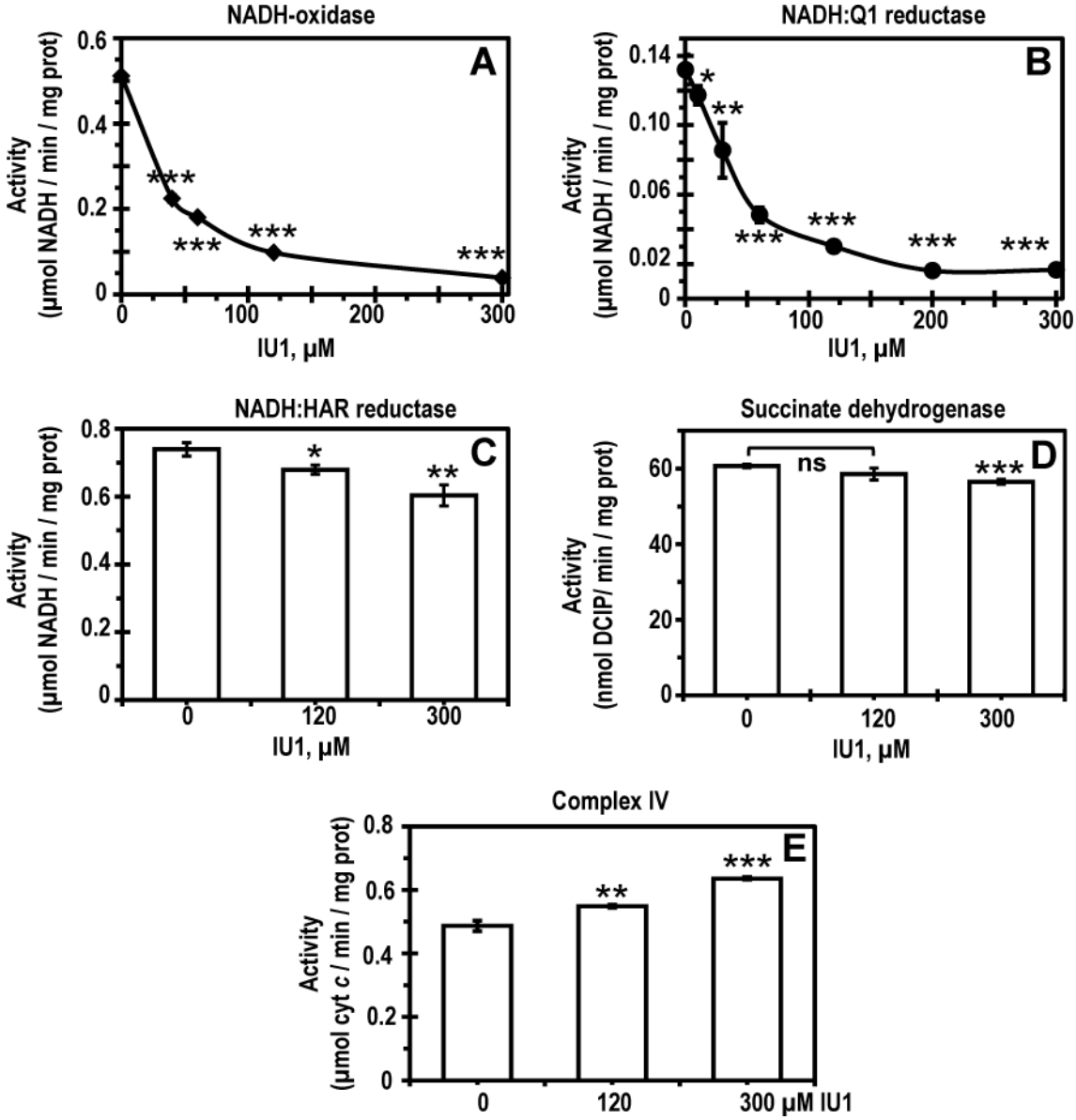

FIGURE 5. Effect of IU1 on mitochondrial respiratory chain complex activities

Permeabilized mitochondrial membranes (2.5–5 µg/ml) from rat brain were pre-treated for 2 min with a range of IU1 concentrations before initiating the reaction by adding the substrates. The activities of Complex I NADH oxidase (A) and NADH:Q_1 reductase (B), oxidation of NADH by the artificial acceptor hexaammineruthenium (HAR) as NADH:HAR oxidoreductase (C), Complex II succinate-dehydrogenase (D), and Complex IV cytochrome *c* oxidase (E) were measured spectrophotometrically at 30°C as described under "Materials and Methods". Activities are expressed in µmol of substrate×min^{-1}×mg^{-1}. Reported values are the mean ± S.D. of at least 3 independent experiments. Asterisks identify values that are significantly different from control (** $p<0.01$; *** $p<0.001$); ns, not significantly different.

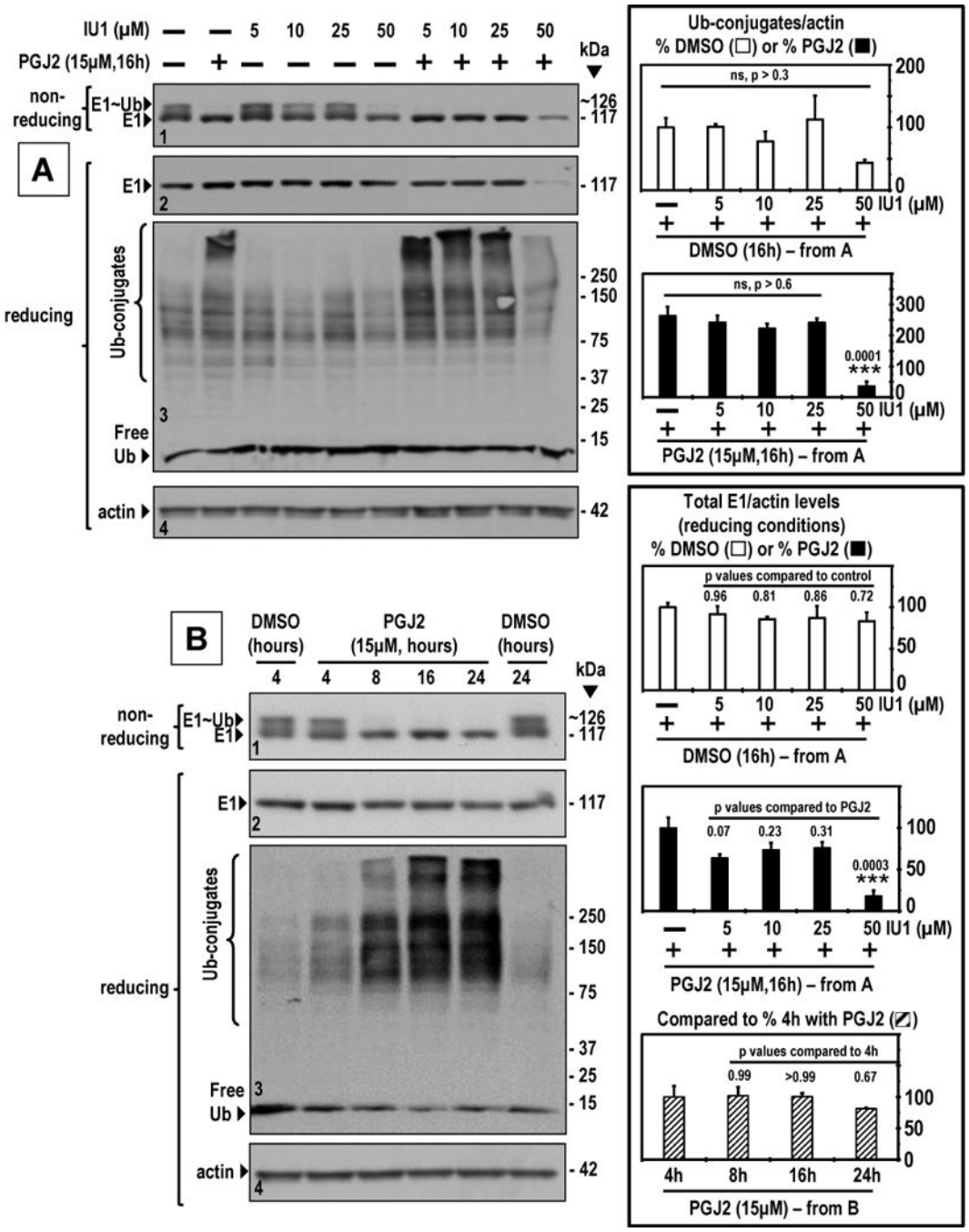

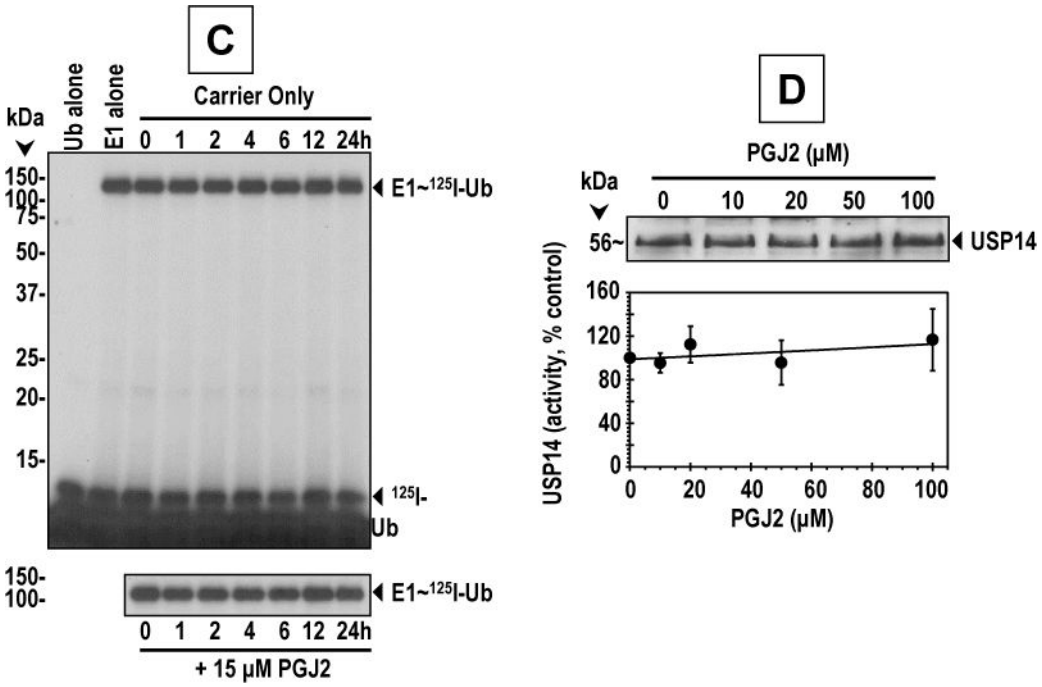

FIGURE 6. Effects of IU1 and PGJ2 treatment (alone or as co-treatment) on the levels of E1~Ub thioester and E1, Ub-proteins and free Ub in rat cerebral cortical neurons and on E1 activity and USP14 *in vitro*

Neurons were treated for 16h in **(A)** with DMSO (vehicle, control), PGJ2 alone (15 μM), different concentrations of IU1 alone (5 μM to 50 μM), or PGJ2 combined with IU1. Graphs on the bottom right represent E1 protein levels (E1~Ub thioester + native E1) semi-quantified by densitometry. Data represent the percentage of the pixel ratio for E1 (under reducing conditions) over actin for each condition compared to DMSO control (100%, *top graph*, all non-significantly different, p values shown for each condition) or PGJ2 alone [100%, *middle graph*, all non-significantly different except for ***, p values shown for each condition]. Values are means from three independent experiments ± s.e. (standard error). In (A, *panel 3*), all the *p* values (*n=4*) determined by comparing Ub-protein levels in control or PGJ2-treated neurons with those when IU1 (5 μM to 50 μM) was added were >0.3, thus non-significantly different, except that PGJ2 + 50 μM IU1 induced a major down-regulation of Ub-proteins compared to PGJ2 (*p=0.0001*). Unconjugated (free) ubiquitin and actin levels (*panels 3 and 4, respectively*) were not decreased by IU1. In **(B)** neurons were treated with PGJ2 alone (15 μM) for different times (4 h to 24 h). Similar data were obtained in three independent experiments. Data represent the percentage of the pixel ratio for E1 (under reducing conditions) over actin for each condition compared to PGJ2 (4h, 15 μM, 100%, all not significantly different, p values shown for each condition). Values are means from three independent experiments ± s.e. (standard error). For (A) and (B) total lysates were analyzed by western blotting (30 μg of protein/lane) probed with the respective antibodies to detect: E1~ubiquitin (Ub) thioesters (*upper bands, panel 1*) and native E1 (*lower bands, panel 1*) run in parallel under non-reducing conditions, or reducing conditions with β-mercaptoethanol (*panel 2*); ubiquitinated (Ub)-conjugates and free unconjugated ubiquitin (Free Ub) (*panel 3*), or actin (loading control, *panel 4*). Molecular mass markers in kDa are shown on the right. In **(C)** E1 activity was assessed in vitro as described under ‘Materials and Methods”.

E1~^{125}I-ubiquitin thioesters (*upper band, top panel; and bottom panel*) were resolved from free ^{125}I-ubiquitin (*lower band, top panel*) under non-reducing conditions by 12% SDS-PAGE at 4°C and visualized by autoradiography. In **(D)** USP14 ubiquitin hydrolase activity was assessed in vitro with HA-Ub-VME as described under “Materials and Methods”. Values in the graph indicate means and s.e. from three independent experiments. There is no significant difference from control (DMSO, 100%).

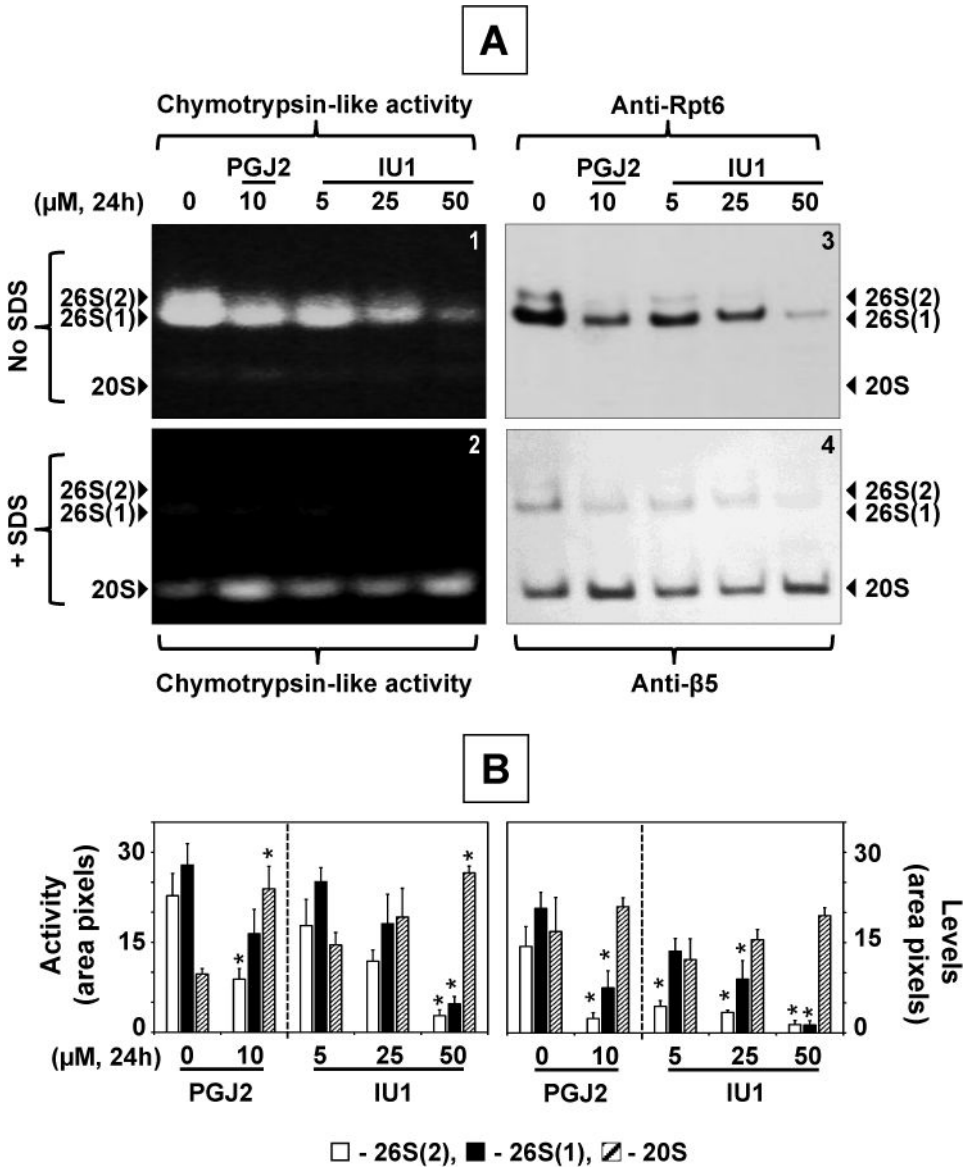

FIGURE 7. Effects of different concentration of IU1 (5 μM to 50 μM) or PGJ2 (10 μM) on proteasome activity and levels in rat cerebral cortical neurons

Neurons were treated for 24 h with increasing concentrations of IU1 or PGJ2. **(A)**, Total lysates were analyzed by the in-gel assay (30 μg/sample) to assess 26S and 20S proteasome chymotrypsin-like activity with the substrate Suc-LLVY-AMC (*panels 1 and 2*), as described under "Materials and Methods". To improve detection of 20S proteasome activity, 0.04% SDS was added to the reaction buffer (*panel 2*). Proteasome levels were detected by immunoblotting with anti-Rpt6 (*panel 3*) and anti-β5 (*panel 4*) antibodies. Arrows on the left and right indicate assembled 26S and 20S proteasomes. **(B)**, Proteasome chymotrypsin-like activity (*left graph*) and levels (*right graph*) were semi-quantified by densitometry (*graph*). Values represent the total number of pixels within each band area divided by one thousand. PGJ2- and IU1-treated samples were compared to the same control (DMSO) sample. Values

are means from at least three independent experiments. Asterisks identify values that are significantly different from control (at least *$p<0.05$).

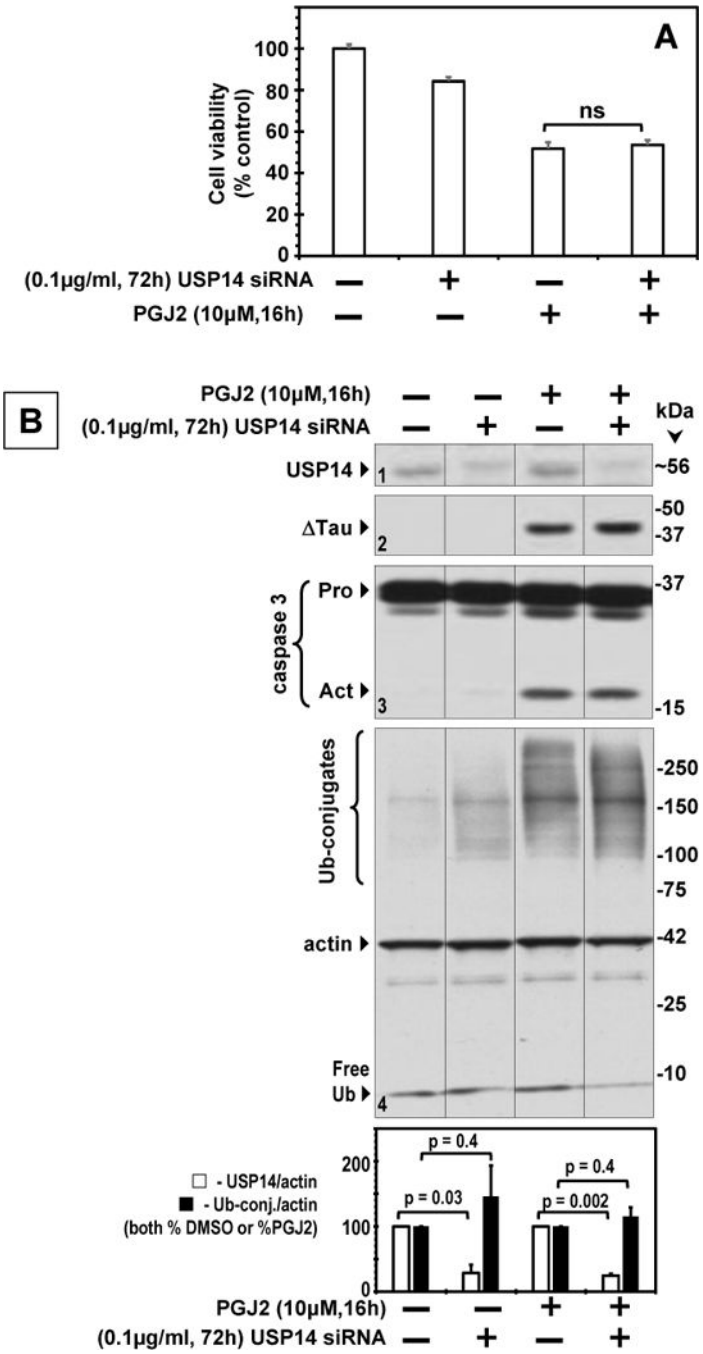

FIGURE 8. Effects of USP14 knockdown by siRNA in rat cerebral cortical neurons

Neurons were incubated with siRNA targeting the *USP14* gene for 72 h, followed by treatment with DMSO (vehicle, control) or 10 μM PGJ2 for 16 h. **(A)**, Neuronal viability was assessed with the MTT assay. Percentages represent the ratio between the data for each condition and control (100%). Values indicate means and s.e. from at least six determinations per group; ns, not significantly different. **(B)**, total lysates were analyzed by western blotting (30 μg of protein/lane) probed with the respective antibodies to detect: USP14 (*panel 1*), caspase-dependent Tau cleaved at Asp421 (Δ Tau, *panel 2*), caspase 3

(*panel 3*), Ub-proteins and free Ub (*panel 4*), and actin (loading control, *panel 4*). Molecular mass markers in kDa are shown on the right. Similar data were obtained in three independent experiments. Pro (full length) and Act (active) caspase 3; Ub, ubiquitinated. USP14/actin (*white bars*) and Ub-protein/actin (*black bars*) levels were semi-quantified by densitometry (*graph*). Values are means from three independent experiments ± s.e. (standard error). P values shown for each comparison.

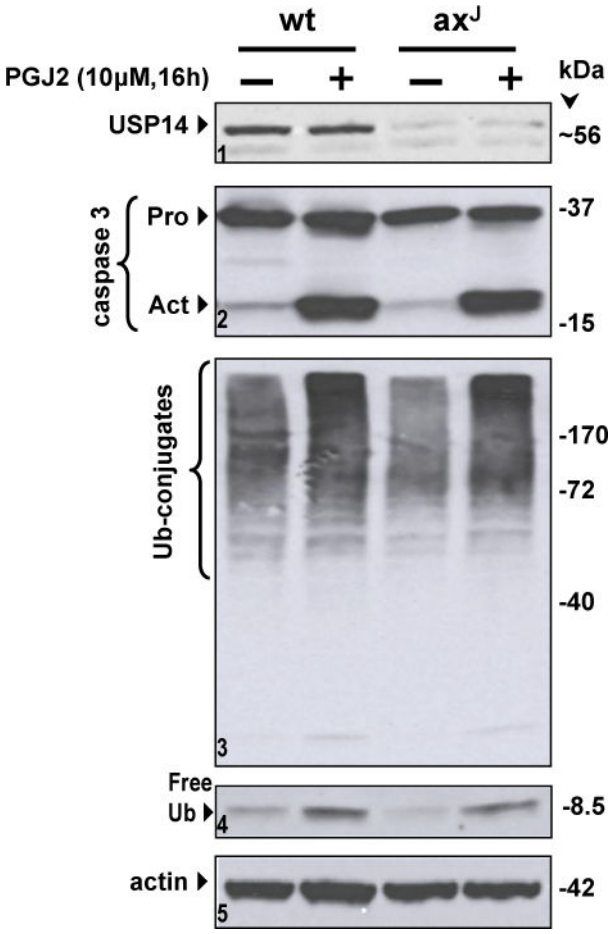

FIGURE 9. Effects of USP14 loss on mouse cerebral cortical neurons

Neuronal cerebral cortical cultures were prepared from wild type (wt) and *Usp14*^{axJ} (*ax*^{J}) mouse brains. Neurons were treated with DMSO (vehicle, control) or 10 μM PGJ2 for 16 h. Total lysates were analyzed by western blotting (30 μg of protein/lane) probed with the respective antibodies to detect: USP14 (*panel 1*), caspase 3 (*panel 2*), Ub-proteins (*panel 3*), free Ub (*panel 4*), and actin (loading control, *panel 5*). Molecular mass markers in kDa are shown on the right. Similar data were obtained in two independent experiments. Pro (full length) and Act (active) caspase 3; Ub, ubiquitin.